**Atmospheric
Chemistry
and Physics**

Analysis of ^{13}C and ^{18}O isotope data of CO_2 in CARIBIC aircraft samples as tracers of upper troposphere/lower stratosphere mixing and the global carbon cycle

S. S. Assonov[1,2,*], **C. A. M. Brenninkmeijer**[2], **T. J. Schuck**[2], **and P. Taylor**[1]

[1]European Commission, Joint Research Centre, Institute for Reference Materials and Measurements, Geel, Belgium
[2]Max Planck Institute for Chemistry, Atmospheric Chemistry Division, Mainz, Germany
[*]presently at: Institute for Geology and Mineralogy, University of Köln, Germany

Abstract. The project CARIBIC (http://caribic-atmospheric.com) aims to study atmospheric chemistry and transport by regularly measuring many compounds in the free troposphere and the upper troposphere/lowermost stratosphere (UT/LMS) by using passenger aircraft. Here we present CO_2 concentrations and isotope results, and analyze the data together with supporting trace gas data. 509 CARIBIC-2 samples (highest precision and accuracy $\delta^{13}C(CO_2)$ and $\delta^{18}O(CO_2)$ data) from June 2007 until March 2009, together with CARIBIC-1 samples (flights between November 1999 and April 2002, 350 samples in total, 270 for NH, mostly $\delta^{13}C(CO_2)$ data) give a fairly extensive, unique data set for the NH free troposphere and the UT/LMS region. Total uncertainty of the data is the same as reported for the global monitoring program by NOAA-ESRL. To compare data from different years a de-trending is applied. In the UT/LMS region $\delta^{13}C(CO_2)$, $\delta^{18}O(CO_2)$ and CO_2 are found to correlate well with stratospheric tracers, in particular N_2O; $\delta^{18}O(CO_2)$ appears to be a useful, hitherto unused, tracer of atmospheric transport in the UT/LMS region and also inter-hemispheric mixing. By filtering out the LMS data (based on N_2O distributions), the isotope variations for the free and upper troposphere are obtained. These variations have only small latitudinal gradients, if any, and are in good agreement with the

data of selected NOAA stations in NH tropics. Correlations between $\delta^{13}C(CO_2)$ and CO_2 are observed both within single flight(s) covering long distances and during certain seasons. The overall variability in de-trended $\delta^{13}C(CO_2)$ and CO_2 for CARIBIC-1 and CARIBIC-2 are similar and are generally in agreement, which underscores agreement between high and low resolution sampling. Based on all correlations, we infer that the CO_2 distribution in the NH troposphere along CARIBIC flight routes is chiefly regulated by uplift and polewards transport of tropical air up to approximately 50° N. The main reason for variability of signals in the troposphere (which is larger for the higher resolution sampling during CARIBIC-2) is mixing of different tropospheric air masses affected by different CO_2 sources and sinks. The effect of stratospheric flux appears to be limited. All in all it is demonstrated that CARIBIC produced new important and reliable data sets for little explored regions of the atmosphere. A logical next step will be global scale modeling of ^{13}C and especially ^{18}O, which is linked to the hydrological cycle.

1 Introduction

The global cycle of CO_2 is of extraordinary complexity and importance. The atmospheric CO_2 reservoir is coupled to those of the oceans, soils, and vegetation and is increasingly burdened by emissions from the combustion of fossil fuel. The significance of CO_2 as a GHG has made documenting

and understanding its atmospheric concentrations, sources and sinks crucial to understanding its influence on climate. Since the extensive paper by Callendar (1938) that dealt with several aspects of the CO_2 cycle including climate effects, many more publications treat nearly all aspects of the "CO_2 problem" in ever greater detail.

Large numbers of observations of CO_2 concentrations at ground-based stations and from ships, aircraft and satellites are made with the goal to tackle the problem of thoroughly understanding and quantifying the large fluxes between the atmosphere and the other reservoirs. The need for large numbers of measurements of atmospheric CO_2 has resulted in, for instance, the North American Carbon Program (http://www.nacarbon.org/nacp/), which involves numerous projects providing a large number of in situ measurements and also vertical profiles provided by tower and aircraft measurements. Besides concentration measurements, flux measurements are carried out, other trace gases are measured for use as proxies of fossil fuel CO_2 (Levin et al., 2008), the O_2/N_2 ratio is measured (Bender et al., 2005), and isotope measurements are conducted. These comprise $^{14}CO_2$ measurements (Levin and Karstens, 2007; Turnbull et al., 2006) and stable isotope measurements (Allison et al., 2007; White and Vaugh, 2009; Vaugh et al., 2010).

There are only a few parameters which, being related to the CO_2 cycle, can be measured directly. Source and sink processes are accompanied by stable isotope fractionation, thus, isotope measurements may provide information about sources and sinks. The first concurrent measurements of atmospheric CO_2 and $^{13}C(CO_2)$ date from before 1960 (Keeling, 1961). The dominant signals contained in the major isotope ratios (i.e. disregarding ^{17}O and clumped isotope signals) are that the $^{13}C/^{12}C$ ratio is dominated by photosynthesis, respiration and combustion whereas the $^{18}O/^{16}O$ ratio is strongly affected by isotope exchange with water, predominantly leaf and soil water. For instance, the large carbon sink of the terrestrial biosphere in the Northern Hemisphere (NH) was confirmed by analyses of gradients in $^{13}C(CO_2)$ (Ciais et al., 1995). For $^{13}C(CO_2)$ even a "flying carpet" or "isolandscape" is available (Vaughn et al., 2010), constructed by the smoothing and interpolation of many such data (Dlugokencky et al., 1994; Masarie and Tans, 1995). A recent paper by Rayner et al. (2008) reports on inverse modeling using $^{13}C(CO_2)$ and CO_2 mixing ratios, and communicates that model improvements and large ^{13}C data sets hold promise here. However, ^{18}O data have not been generated and used to the same degree, and contain different, perhaps more convoluted information that, however, ought to be fully understood and may hold useful applications (Still et al., 2009).

When endeavoring to estimate CO_2 fluxes and transport mixing with confidence, the number of atmospheric observations available worldwide is still limited for crucial regions. Based on data from CO_2 observational networks (Patra and Maksyutov, 2002; Patra et al., 2003) concluded that there exists a need to extend the network by optimally lo-

cated stations in continental South America, Africa and Asia. One of the contributions to help to close the gap is to use aircraft observation platforms (Expert Group Recommendations of 13th_WMO/IAEA_Meeting). In fact, already in 1966 Bischof and Bolin (1966) reported on aircraft based CO_2 measurements.

CARIBIC (Civil Aircraft for the Regular Investigation of the atmosphere Based on an Instrument Container, www.caribic-atmospheric.com) uses a passenger aircraft that on a monthly basis conducts long distance measurement flights using an automated laboratory for real time measurements of trace gases and aerosol and the collection of whole air and aerosol samples for laboratory analysis. Included in the measurement package are measurements of CO_2, which, in view of its great importance as a GHG, have their own weight to help to tackle the "CO_2 problem".

CO_2 and GHG measurements in CARIBIC were, and to a large degree still are, based on the analysis of air samples, although an in situ analyzer for CO_2 is tested in CARIBIC-2. Having air samples available, it is a logical step to conduct stable isotope measurements. Why? First, the overall project represents a significant technological, logistical and scientific effort. As such, the optimization of the scientific payload and its use is essential. Second, to our knowledge there are no other large scale, high accuracy precise systematic CO_2 isotope measurements in the tropical free troposphere and UT/LMS. Conversely, it is also evident that air samples collected at large distances from sources and sinks mostly in background air where signal variability is not large require high quality analyses.

We measured and here present and discuss in detail the results of accurate and precise CARIBIC CO_2 isotope analyses of a wide range of representative air masses, primarily encountered in the northern hemisphere. To generalize this information and to organize the CARIBIC data set, we describe the method of grouping the data according to air mass chemical composition and origin (meteorological regime). Analysis of CO_2 data for a similar aircraft project, CONTRAIL (Matsueda et al., 2002, 2008) appears to be less complicated as CONTRAIL flights do not cross the UT/LMS region. Because the isotopic variability of signals at flight altitudes is rather limited and the type of platform is not used on a large scale either, we present here a more extensive description of our methods, uncertainty and the data handling than would be necessary for discussions of atmospheric constituents more routinely measured. In the following we first give basic information about the CARIBIC platform, followed by details about the mixing and isotope ratio measurements. Second, we show how the time series spanning 1997–2008 can be de-trended, after which we explain those air masses that are sampled and, third, we apply tracer-tracer correlations to demonstrate the effect of UT/LMS mixing by optimal usage of chemical stratospheric tracers. Fourth, we discuss the data of the free tropical troposphere and UT region followed by a comparison of the CARIBIC time series with the extensive

data available from NOAA-ESRL. We demonstrate which details of global CO_2 distribution can be recorded by aircraft.

Finally, we discuss future data use in models and address certain aspects of sampling and model resolution, as well as the quality of analytical data. Comparison between CARIBIC-1 and CARIBIC-2 gives a good example of different resolution approaches. Further developments of isotope measurements by CARIBIC are briefly discussed.

2 Experimental

2.1 The CARIBIC observatory

CARIBIC (http://caribic-atmospheric.com) investigates atmospheric chemistry, transport and composition by measuring many compounds (long and short lived trace gases and aerosol) using an automated laboratory aboard a passenger aircraft, which travels from Europe to a number of different regions of the globe. The monthly flights have taken place over a number of years and cover large regions while measuring many species simultaneously, ultimately providing data sets that are not otherwise available.

The flight tracks, dates and sampling locations are shown in Fig. 1. Nearly all information obtained is for cruise altitude, i.e. between 9 and 12 km. (The lowest sampling altitude was 7 km). From such altitudes little regular, detailed isotope information is available. Each long distance flight covers a wide range of atmospheric regions/regimes, opposite to land-based stations. Cruising in the mid-latitude upper troposphere/lowermost stratosphere and the tropical troposphere means that sampling is remote from CO_2 sources and sinks. However, convection and the larger scale uplift of air masses can at times deliver air parcels with a certain surface air affected component to cruising altitude. To give a number, $\approx 35\%$ of samples analyzed for 2007–2008 were from the UT/LMS at extra-tropical mid-latitudes. An inventory of air masses probed by CARIBIC-2, based on cluster analyses is given by Köppe et al. (2009). Schuck et al. (2009) presents CO_2 and other greenhouse gas data, whereas a brief overview for CARIBIC-1 is given by Zahn et al. (2002).

CARIBIC-1 operated from late 1997 until April 2002, using a Boeing 767 (LTU, Germany), sampling on routes to and from the Maldives, Sri Lanka, Southern Africa, and the Caribbean. Each month 12 large air samples of nominally ≈ 340 L STP were collected during one flight leg (Brenninkmeijer et al., 1999). Each air sample represented a flight distance of ≈ 250 km. An initial overview of CARIBIC-1 isotope data was given by Assonov et al. (2007), whereas details of isotope measurements and calibration are published in (Assonov et al., 2009b).

CARIBIC-2 started its operation in early 2005 and is based on an Airbus A340-600 from Lufthansa Airlines equipped with a sophisticated air inlet system and carrying a totally new container (1.5 ton) with a multitude of analyzers (Brenninkmeijer et al., 2007). Here 28 samples are collected each month, with the samples being collected during all 4 flight legs or only during the first 2 flight legs. Under typical sampling conditions, these samples are collected over a period of ≈ 45 s, corresponding to a sampling distance of ≈ 15 km. Details of the sampling system and procedure are given by Schuck et al. (2009). Like in CARIBIC-1 the collection of samples and all (online) measurements are fully automated with air sampling conducted at fixed time intervals fairly evenly spaced along the flight track. Details of isotope measurements and calibration for CARIBIC-2 are published by Assonov et al. (2009a). CARIBIC-2 data from between April 2007 and March 2009 (21 flights which is the subset used for CO_2 isotope analyses), represents the latitudes 14 to 55° N, with some flights to North America and one to South Africa, but mostly flights to the Philippines and India.

2.2 Concentration and isotope measurements

The CO_2 mixing ratios are based on gas chromatography (GC) with simultaneous measurement of CH_4, N_2O and SF_6. The analytical procedure and performance for CARIBIC-2 are given in detail by Schuck et al. (2009). The measurement precision (as based on measurement repeatability) and combined measurement uncertainty (obtained using individual measurement uncertainties and those associated with calibration, instrumental and other corrections) for CO_2 are about 0.15 and 0.20 ppm respectively. For CARIBIC-1 no account has been published. Based on years of the GC performance, the precision and combined measurement uncertainty for that period are assessed to be 0.20 and 0.25 ppm. CO_2 concentration measurements are traced back to the WMO X2007 scale for CO_2-in-air using NOAA-ESRL primary standards.

The CO_2 isotope analyses for CARIBIC-1 and CARIBIC-2 differ in many aspects, namely the aircraft sampling system, sample size, mass spectrometry and correction procedures. CARIBIC-1 samples were analyzed at MPI-C, Mainz (Assonov et al., 2009b), 100% efficiency of the CO_2 extraction procedure demonstrated by Pupek et al. (2005); CARIBIC-2 samples were analyzed at JRC-IRMM, Belgium (Assonov et al., 2009a). In both cases proper calibration vs NBS-19-CO_2 was confirmed by excellent agreement with NIST RMs CO_2 and NARCIS-CO_2. For CARIBIC-2, an inter-comparison with MPI-BGC demonstrated a small, consistent scale discrepancy in δ^{13}C(CO_2) of $-0.04\permil$ and δ^{18}O(CO_2) of $-0.06\permil$ (Assonov et al., 2009a). This is much less than the variability discussed in the present paper, and less than inter-laboratory scale discrepancies recently published, which reach $0.08\permil$ for δ^{13}C(CO_2) and $0.4\permil$ for δ^{18}O(CO_2) (e.g. Levin et al., 2007).

Typical combined measurement uncertainties of the CARIBIC-1 and CARIBIC-2 CO_2 data (obtained using the measurement uncertainties associated with uncertainties of individual measurements, calibration measurements, instrumental and other corrections, the uncertainty budget given by
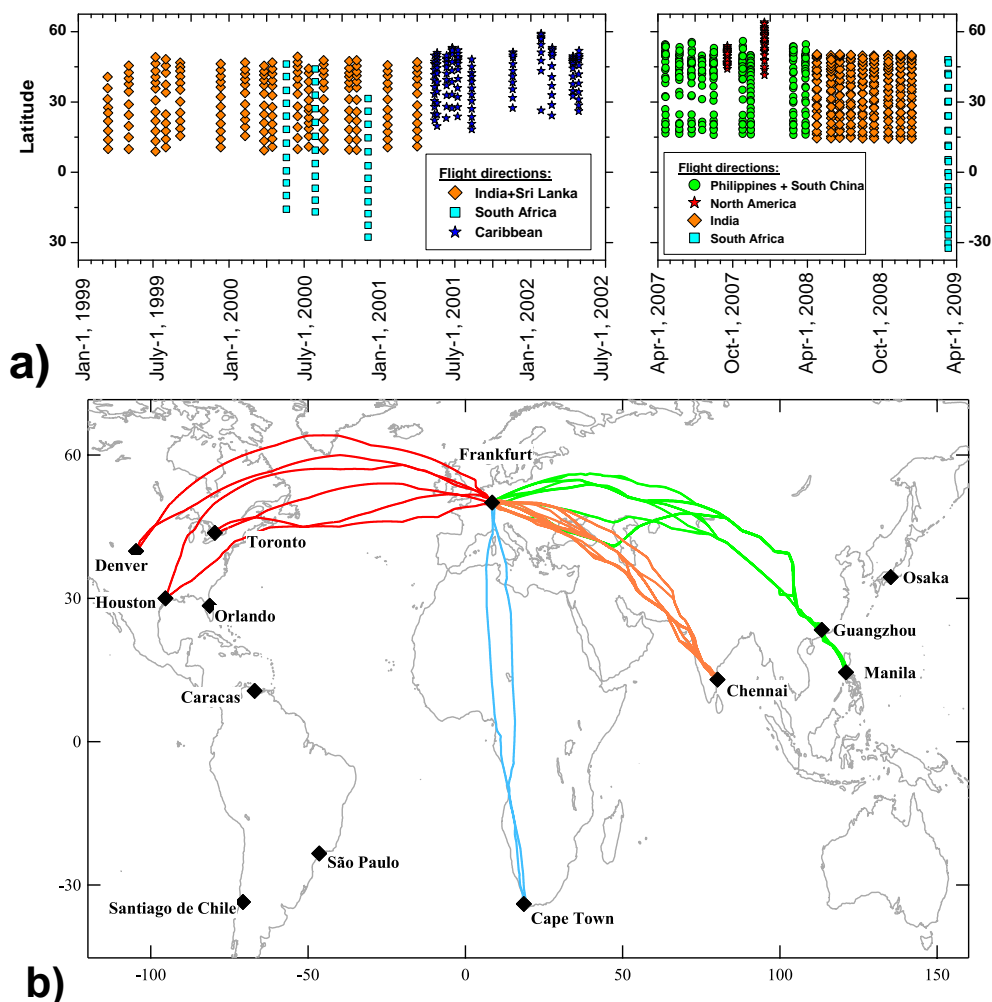
Fig. 1. (a) CARIBIC-1 and CARIBIC-2 sample distribution used for CO_2 isotope analyses; **(b)** CARIBIC-2 flight routes.

Assonov et al. (2009a) based on Brand et al., 2010) are given in Table 1. Though the combined uncertainty for our isotope data exceeds the inter-laboratory compatibility targets set at 0.01‰ for $\delta^{13}C(CO_2)$ and 0.05‰ for $\delta^{18}O(CO_2)$ (Expert Group Recommendations of 13th_WMO/IAEA_Meeting), the data appear to be one of the best achieved to date. NOAA-ESRL have measurement precision of 0.01‰ and a combined measurement uncertainty of 0.02‰ for $\delta^{13}C(CO_2)$ (all values given as 1-σ), with the values of 0.03 and 0.07‰ for $\delta^{18}O(CO_2)$ correspondingly; the $\delta^{13}C(CO_2)$ accuracy estimated on inter-laboratory comparisons (the meaning appears to be close to the compatibility of measurement results as introduced by VIM 3) is 0.03‰ (White and Vaughn, 2009). All in all, the combined measurement uncertainty for $\delta^{13}C(CO_2)$ and $\delta^{18}O(CO_2)$ for CARIBIC data (Table 1) is the same as the uncertainty obtained at NOAA-ESRL.

Table 1. Typical combined uncertainty (1-σ values) of the CARIBIC-1 and CARIBIC-2 CO_2 measurements and for measurements at NOAA-ESRL (Conway et al., 2009; White and Vaughn, 2009).

	CO_2, ppm	$\delta^{13}C(CO_2)$, ‰	$\delta^{18}O(CO_2)$, ‰
CARIBIC-1	0.25	0.022	0.063
CARIBIC-2	0.20	0.020	0.030
NOAA-ESRL	0.20	0.020	0.070

Isotope exchange between CO_2 and traces of H_2O is a known problem that leads to artifacts of more negative $\delta^{18}O(CO_2)$ values (e.g. Masarie et al., 2001). In CARIBIC-1 where stainless steel canisters of 20 liter at ≈ 17 bar were used the data showed the problem of exchange. This improved in time, but persisted for some cylinders. The

CARIBIC-1 results used are filtered according to negative $\delta^{18}O(CO_2)$ deviations (Assonov et al., 2009b). As the remaining $\delta^{18}O(CO_2)$ data still might have been affected to a small but undefined degree (after October 2000 data are more reliable, see Assonov et al., 2009b), the CARIBIC-1 $\delta^{18}O(CO_2)$ data are used qualitatively only.

In CARIBIC-2 glass flasks at ≈ 4 bar are used and no effects of ^{18}O exchange between CO_2 and H_2O were detected. Only two samples were suspect at the beginning of measurements at IRMM (presumably problems of gas extraction) and their data rejected. Independent proof of absence of isotope exchange in glass flasks under aircraft conditions would require tests for which the means were not available. The frequency distribution of the values obtained and the literature on the use of glass flasks, given the fact that air at cruise altitude is very dry, lend credibility to the assumption that no exchange in excess of measurement error has occurred. Moreover, several longer term storage tests showed only small $\delta^{18}O(CO_2)$ shifts.

Scale consistency for $\delta^{13}C(CO_2)$ is a great concern (Expert Group Recommendations of 13th_WMO/IAEA_Meeting, 2005; Allison and Francey, 2007; Vaughn et al., 2010). All CARIBIC-2 data are on the VPDB-CO_2 scale (linked to NBS-19-CO_2) by using the ^{17}O correction by Assonov and Brenninkmeijer (2003) which is currently being officially recommended (Brand et al., 2010). The NOAA-ESRL data used in the paper being produced using the ^{17}O correction by Allison et al. (1995) and the CARIBIC-1 data (Assonov et al., 2009b) produced using same ^{17}O correction are now corrected for the differences between the algorithms (Assonov – Allison) which can be approximated by

$$\Delta[\delta^{13}C(CO_2)] = -[0.0031 \cdot \delta^{18}O(CO_2) + 0.030‰] \qquad (1)$$

From 2009 onwards NOAA data are generated using the ^{17}O correction by Assonov and Brenninkmeijer (2003), see (Vaughn et al., 2010).

Finally, 28 samples from a flight in March 2009 were analyzed at MPI-BGC using the same method as used at JRC-IRMM; the data obtained are corrected for the interlaboratory scale discrepancy we have observed.

3 Observational data

3.1 Meteorology and trace gas measurements: aspects specific for civil aircraft sampling with an overview of GHG data

CARIBIC data are gathered at different latitudes and longitudes (Fig. 1a, b) within a narrow range of altitudes. One single flight covers a wide range of meteorological regimes such as mid-tropospheric air in the tropics or upper tropospheric air and lower stratospheric air in mid- and high-latitudes. The cruise altitude during a single flight usually increases with fuel consumed, and typically ranges from 9 to 12 km.

The typical pressure altitude for CARIBIC-1 (Boeing 767) was 266 ± 25 hPa (Median and 1 StDev). For CARIBIC-2 (Airbus A340-600) this was 237 ± 33 hPa. Most CARIBIC instruments operate only at pressure altitudes of 500 hPa or less (higher altitude) to avoid contamination of the sensitive analytical systems and for this reason limited vertical profile information is available.

At mid-latitudes, flights cross the tropopause and lowermost stratospheric air is frequently sampled. At lower latitudes where the tropopause is higher, free tropospheric sub-tropical and tropical air is encountered. We note that the return flights over Europe reach deeper into the LMS than forward flights (due to altitude increasing during the flight). During return flights meteorological conditions are usually similar to those of the outbound flights, so that GHG and other profiles of forward and return flights nearly mirror each other. Relevant meteorological parameters (5 day back trajectories, potential vorticity cross sections along the flights, etc.) for all CARIBIC flights are available at the KMNI web-site (http://www.knmi.nl/samenw/campaign_support/CARIBIC/). An example of analyses of meteorological parameters, and chemical tracers by CARIBIC-1 is given in (Zahn et al., 2002).

Many trace gases are measured from the air samples, but here we discuss, in addition to CO_2, $\delta^{13}C(CO_2)$ and $\delta^{18}O(CO_2)$ and where applicable, only the main greenhouse gases namely CH_4, N_2O and SF_6. Figure 2a, b gives the 4 scatter plots for CARIBIC-2 against O_3 for which the data from continuous recording were integrated over the sampling intervals. For CO_2, CH_4, N_2O and SF_6 one can discern mixing trends towards LMS air (high O_3) with a large variability for tropospheric air masses (O_3 values typically below 100 ppb). For N_2O tropospheric variability is lowest. For SF_6 the relative uncertainty is lowest, but the scatter for tropospheric samples is large, mostly due to the effect of its localized sources. For that reason CH_4 also shows tropospheric scatter, but otherwise has a compact UT/LMS mixing line. CO_2 concentrations demonstrate the largest variability for tropospheric air masses mainly due to its seasonal cycle. All these gases but methane have increasing trends. The seasonal variability propagates into the lowermost stratosphere while being continuously attenuated by ongoing mixing with LMS air. Below we demonstrate how CO_2 isotope data reflect the two dimensions of variability, namely in the mixing trend towards LMS air and in tropospheric air masses.

We also show in Fig. 2c, d by using sampling interval integrated continuous CO values, the O_3 excess vs. the chemical tropopause as defined by Zahn et al. (2004b) and N_2O (detrended data) vs. CO as well as histograms of O_3 and N_2O distribution (Fig. 2e, f). For discriminating between tropospheric and stratospheric samples one can, in principle, use physical tracers (e.g. PV values) or one of the chemical tracers N_2O, SF_6, CH_4 and O_3. Later in the manuscript we will select the most suitable tracer for this purpose, namely detrended N_2O data.
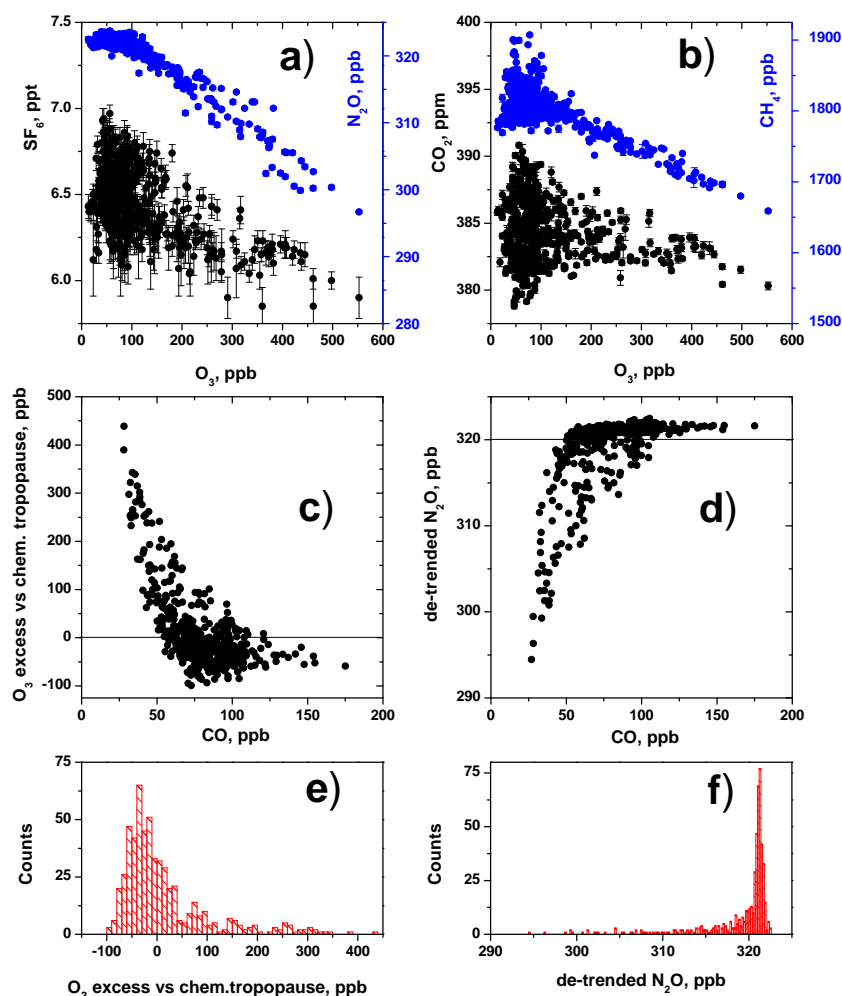
Fig. 2. (a–b) GHG data (N_2O, SF_6, CH_4 and CO_2) for CARIBIC-2 flights from April 2007 to March 2009 (period covered by CO_2 isotope analyses) plotted against ozone. The data are not de-trended and all samples (tropical free troposphere, UT and LMS) are all plotted together. **(c–d)** Comparison of stratospheric tracers O_3 and N_2O. De-trended N_2O data vs. CO demonstrate a more compact distribution for tropospheric air masses (N_2O above 320 ppb) than the distribution of O_3 vs. CO. (Tropospheric air may be distinguished as having O_3 excess vs the chemical tropopause above zero). **(e-f)** histograms of O_3 and N_2O distribution.

3.2 Data de-trending

For comparing CARIBIC-1 and CARIBIC-2 CO_2 data, which together cover 10 years with a break of about 5 years, a de-trending is necessary to account for the trends in CO_2, $\delta^{13}C(CO_2)$ and N_2O. We base the de-trending factors (Table 2) on the NOAA flask data obtained for remote stations in the NH tropics. (We use the N_2O obtained by NOAA on the same flask samples as used for CO_2 and $\delta^{13}C(CO_2)$). First, monthly means were used to obtain annual averages, upon which, for CO_2 and N_2O, the average slopes of the linear fits are established. In this way all CARIBIC data are de-trended to 1 January 2007.

The de-trending procedure introduces errors which are manifest as deviations from the fit lines (Fig. 3a, b, c). The linear fit for CO_2 captures nearly all of the variance over the

years of interest (J. White, personal communication, 2009) with deviations between -1 to 0.5 ppm. Therefore higher order fits (Masarie and Tans, 1995) are not applied.

As trends in CO_2 and $\delta^{13}C(CO_2)$ are caused by common source and sink processes, the $\delta^{13}C(CO_2)$ decrease must be consistent with the inferred CO_2 increase. Plotted are $\delta^{13}C(CO_2)$ vs. the inverse of the CO_2 concentration (Fig. 3b) for representative background stations MLO and KUM, which have uninterrupted records. Combination of this $\delta^{13}C(CO_2)$ trend and the CO_2 increase rate (Table 2) results in an annual $\delta^{13}C(CO_2)$ decrease rate. The trends for these remote stations agree well (for MLO and KUM the intercepts of -14.2 and -14.0‰). Plotting $\delta^{13}C(CO_2)$ vs year (not shown) gives basically the same slope but this cannot demonstrate a consistency between $\delta^{13}C(CO_2)$ and CO_2 increase rates. Because trends in CO_2 and $\delta^{13}C(CO_2)$
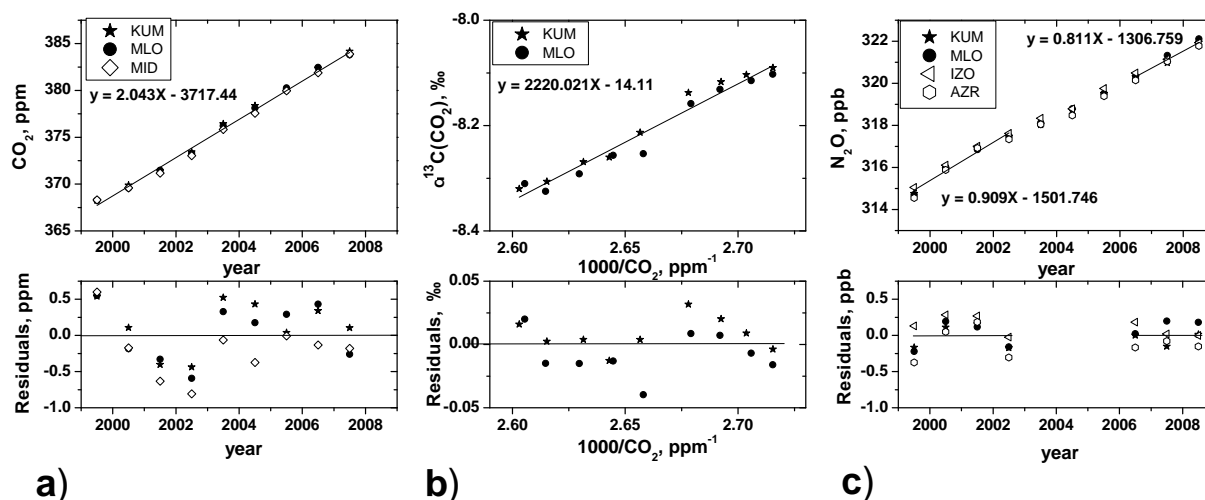
Fig. 3. Linear fits through annual means of CO_2 **(a)**, $\delta^{13}C(CO_2)$ **(b)** and N_2O **(c)** for selected background NOAA stations (see Table 2). Residuals are shown in lowermost panels. To demonstrate the consistency between the $\delta^{13}C(CO_2)$ increase rate with the CO_2 increase, the $\delta^{13}C(CO_2)$ trend vs. $1/CO_2$ has been used, see text.

Table 2. Annual increase rates (linear fits) for the NOAA stations.

Variable	Stations	Data source	Years	Increase rate
CO_2	MLO, KUM, MID	NOAA ftp server (Conway et al., 2009)	1999–2007	2.04 ppm/y
$\delta^{13}C(CO_2)$	MLO, KUM	NOAA ftp server (White and Vaughn, 2009)	1999–2007	−0.032‰/y
N_2O	MLO, KUM, IZO, AZR (flask samples)	NOAA (Dlugogencky, 2009)	1999–2002 2006–2008	0.909 ppb/y 0.811 ppb/y

are linked by source/sink processes, and because analytical errors in $\delta^{13}C(CO_2)$ are close its annual change, the $\delta^{13}C(CO_2)$ decrease must be checked for consistency with the CO_2 increase. For the same reason de-trending cannot be applied for the years of CARIBIC-1 and CARIBIC-2 separately – slopes of trends for 3–4 years vary significantly, depending on the years included. Only 6 year or a longer trends can give a robust slope estimate.

Errors for the $\delta^{13}C(CO_2)$ de-trending are not easily quantified. First, the annual $\delta^{13}C(CO_2)$ decrease is nearly of the same magnitude as the long term measurement accuracy. Second, the variability of seasonal circulation patterns (e.g. discussed for CO_2 at Mauna Loa, Lintner et al., 2006) causes variability in air mass composition and CO_2 signals at stations. The first estimate of errors may be given by $\delta^{13}C(CO_2)$ deviations relative to the linear fit, which are mostly within 0.025‰, with one value deviating by about 0.05‰ (Fig. 3b).

Two linear fits for N_2O station data (Fig. 3c) were applied, separately for the years of CARIBIC-1 and CARIBIC-2 (Table 2). The mean fit slopes are 0.909 and 0.811 ppb/y (Table 2, years 1999–2002 and 2006–2008) appears to agree with values obtained over 1994 to 2006 for several NOAA

stations (a range from 0.76 to 0.85), with a global cosine-weighted average of 0.80 (Jiang et al., 2007). Deviations from the linear fits do not exceed 0.5 ppb (Fig. 3c). CARIBIC-1 data being first de-trended for 1 January 2002 were then shifted to a common level with CARIBIC-2 (de-trended for 1 January 2007), by applying the shift determined from station data. De-trended monthly means for the stations MLO, KUM, IZO, AZR (years 1999–2002 corrected for the shift between de-trending for 11 January 2002 and 11 January 2007) show nearly identical distributions, with Medians of 320.8 ppb and 1 StDev. of 0.3 ppb (Fig. 4a). The distributions are slightly skewed, possibly due to the anomalous increase of N_2O in 2000 and 2001 (Fig. 3c, see also Jiang et al., 2007). Here, variability in air mass composition (e.g. Mauna Loa, Lintner et al., 2006) may also play a role. The distribution widths include both seasonal variations and errors introduced by data de-trending. The fact that several stations in the NH tropics have narrow and nearly identical distributions of N_2O, with maximal deviations from the Median within 0.9 ppb (3-σ), implies that the N_2O distribution can be used to construct the filter applied to separate tropospheric air from the LMS air discussed in the following.
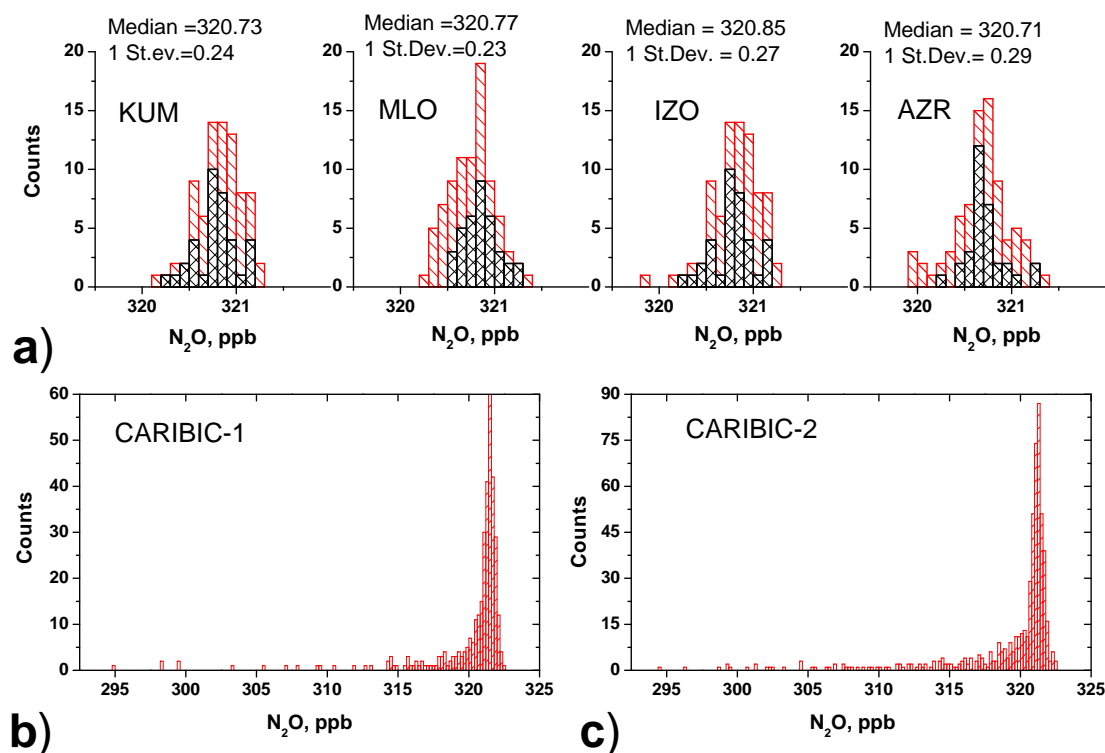
Fig. 4. (a) Distribution of de-trended, monthly mean N_2O data for NOAA stations in the NH tropics, 1999 to 2002 (in red) and 2006 to 2008 (in black). The distributions have the same Median at 320.8 ppb and very similar widths. **(b–c)** Distribution of ozone data and de-trended N_2O data for CARIBIC-1 and CARIBIC-2. Majority of samples represent tropical free tropospheric and UT air masses and have N_2O above 320.0 ppb; the tailing to lower N_2O values is due to the contribution of LMS air masses.

3.3 Use of tracers to distinguish LMS air masses from tropospheric air masses

In order to analyse the results, the CARIBIC-1 and CARIBIC-2 data are separated in two pools representing (i) tropospheric air, i.e. free troposphere plus upper troposphere air masses, and (ii) LMS air and air masses resulting from UT/LMS mixing processes. Because CARIBIC covers different latitudes, altitudes and seasons, and high resolution samples are collected, choosing an appropriate separation criterion is not trivial. CO_2 is a long lived tracer and each sample typically contains an air mixture of different history. Back-trajectories of 5 or 8 days as commonly used in CARIBIC chemical studies are not sufficiently informative, whereas prolonged back-tracking of air masses makes little sense in view of uncertainties in transport and mixing. Using modeled PV values demonstrates a large scatter (not plotted), with occasional values of up to 5 PV for air masses which are considered to be tropospheric based on O_3 being below the chemical tropopause and high N_2O.

Whereas pure meteorological tropopause definitions (like PV) may not have the required resolution, the chemical tropopause is an operational concept based on gradients of contrasting tracers measured in situ. Using the stratospheric tracer O_3 and the contrasting tropospheric tracer CO (typi-

cally giving the compact curvilinear mixing relationship, in UT/LMS publications often named L-shape mixing plots, cf. O_3 vs. CO, Fig. 2c), Zahn et al. (2004b) introduced an ozone based chemical tropopause with a seasonally varying boundary level of O_3. Different groups (Pan et al., 2004; Hoor et al., 2004, 2005) also demonstrated that use of chemical tracers and the chemical tropopause is truly informative to describe mixing of air masses of different origin in the UT/LMS region. The applicability of chemical tracers was even proven in case of double thermal tropopause occurrences in the extra-tropics (Pan et al., 2007).

For discrete UT/LMS events of CARIBIC-1 it was shown that $\delta^{13}C(CO_2)$ correlated well with the O_3 excess vs. the chemical tropopause (Assonov et al., 2007). However, due to a limited data set, low sampling resolution and problems with flasks, the same was not shown for different seasons and $\delta^{18}O(CO_2)$. In particular, O_3 variability and seasonality in the LMS as well as mixing structures (stratospheric intrusions and fine filaments of stratospheric air) may play a role. For such mixing structures O_3 data may not be a sensitive indicator (e.g. Hocking et al., 2007). When aiming to construct a robust filter to separate LMS air masses for the high resolution CARIBIC-2 data set, the use of O_3 needs to be compared with another suitable candidate, namely N_2O. An obvious

reason to consider N_2O is that its lifetime better matches that of CO_2 than that of O_3; besides, N_2O was measured directly from the air samples. At the outset there are some disadvantages associated with the use of O_3. i) Stratospheric O_3 has a seasonal variability due to production changes (e.g. Hegglin and Shepherd, 2007), whereas the long lifetime of N_2O results in a gradual destruction only. Indeed, N_2O plotted vs. O_3 for CARIBIC-2 (Fig. 2a) shows a clear variability of slopes at higher O_3 values; ii) Photochemical production and destruction of O_3 in the troposphere (Zahn et al., 2002) leads to variability as well. This is visible in Fig. 2c–d and histograms (Fig. 2e–f) – the peak at O_3 below the ozone tropopause level is not as compact as the peak at N_2O above 320 ppb. Some samples having low O_3 (accordingly classified as UT air) also have low N_2O (not plotted) and must actually be considered to be LMS air. Conversely, some samples with O_3 in excess of the chemical tropopause level, also have high N_2O, and thus are definitely tropospheric.

In contrast to O_3, N_2O demonstrates a compact and narrow peak at high N_2O above 320 ppb (Fig. 2d, f) with tailing towards lower values corresponding to the LMS contribution. This as well as the narrow distribution of N_2O for background air at tropical NH stations (Fig. 4a) implies that a certain N_2O level may be used as a cut-off providing a robust filter for LMS and LMS-affected air masses. There are compelling reasons to use N_2O. i) N_2O has been successfully used to describe the UT/LMS mixing (Hoor et al., 2004), we cite: "... tropospheric N_2O is well mixed giving a rather constant tropospheric mean value... It's major sink is in the tropical stratosphere where it is destroyed via photolysis and reaction with $O(^1D)$. The long local photochemical lifetime... leads to much weaker N_2O-gradients at the tropopause than for O_3, but makes it ideal to trace stratospheric transport since N_2O is not affected by local photochemistry..."; ii) CO_2 oxygen isotope changes in the stratosphere correlate better with N_2O than with O_3 (Boering et al., 2004). These authors consider N_2O as a tracer giving an effective reaction time for CO_2 oxygen isotope changes; iii) N_2O data are obtained from the same air samples as used for CO_2 isotope analysis, which excludes any uncertainty related to integration of continuous ozone data over the sampling interval.

Despite N_2O offering advantages, its application has been limited for chiefly two reasons: (i) high precision N_2O measurements, being lab based using flask samples, are rare, whereas O_3 data are obtained routinely at high resolution; (ii) the ratio of O_3 variability to precision is about 500 (range 500 ppb, precision 1 ppb), whereas the ratio for N_2O is only about 80 (range 25 ppb, precision 0.3 ppb).

When using N_2O one has to decide on the appropriate cut-off level. The distribution for CARIBIC-2 (de-trended to 1 January 2007) has a distinct peak with the Median at 321.2 ppb (Fig. 4b, c). Although a cut-off of 320.0 ppb is selected arbitrarily, this is a safe approach – the distance (the peak Median minus the cut-off level) being 1.2 ppb slightly exceeds both the half-width of the CARIBIC peak

and the maximal seasonal variability of N_2O in the NH tropics (3-σ of 0.9 ppb, Fig. 4a). CARIBIC-1 data (de-trended as discussed above) show the same features.

4 Discussion

4.1 CO_2 isotope data for LMS air masses

4.1.1 Examples of flights that sampled LMS air masses

CARIBIC-2 flights crossing LMS air masses have recorded detailed correlations for a range of trace gases (Fig. 5). Such events are well recorded by concomitant CO and O_3 values reflecting UT/LMS mixing (compact curvilinear mixing relationship), but also by lower N_2O, CH_4 and SF_6 values. At times detailed and clear compact curvilinear mixing relationships (similar to the curvilinear mixing relationship, also known as L-shaped O_3 vs. CO plots) are obtained for CO_2, $\delta^{13}C(CO_2)$ and for $\delta^{18}O(CO_2)$, (Fig. 5, data given vs. N_2O reversed scale) implying that UT/LMS mixing can be reflected by CO_2 isotopes. (Compositions of UT and tropospheric end-members define the compact curvilinear mixing relationship, namely a folded trend line). Such correlations due to UT/LMS mixing have been observed for 14 out of 21 flights.

As pointed out, outward and corresponding return flights usually cross nearly the same stratospheric structures (folds, intrusions and filaments), resulting in nearly symmetrical PV and GHG profiles. In such cases the UT/LMS mixing lines for CO_2, $\delta^{13}C(CO_2)$ and for $\delta^{18}O(CO_2)$ (or some of the signals) start from the same stratospheric end-member. Notably, GHG plots for outward and corresponding return flights mirror each other (Fig. 5). A large variability in the composition of tropospheric air masses over a single flight is often observed, implying a variety of air masses taking part in the LMS ventilation and/or the UT air masses mixed-in/transported directly to this region.

By binning CARIBIC-2 flights that probed the UT/LMS in 4 seasons (Fig. 6, only latitudes above $35°$ N are plotted), one can observe a similarity of the stratosphere-enriched end-member's composition, with somewhat variable degree of this enrichment (lowest N_2O in different seasons is different), while the variability of the slopes of the mixing trend lines is large. The latter strongly depends on the variability and/or seasonality of UT component(s), while also a variable regime of LMS ventilation (Zahn et al., 2004a) plays a role. Thus different stratospheric enrichment recorded in different seasons might also be due to variable thickness of the LMS mixing reservoir and variable altitude of the tropopause. The CO_2 and $\delta^{13}C(CO_2)$ plots appear to be nearly perfect mirror images, which is expected because $\delta^{13}C(CO_2)$ vs. $1/CO_2$ in the troposphere are linked by source and sink processes. The $\delta^{18}O(CO_2)$ plot shows positive slopes for all seasons (reasons will be explained below).
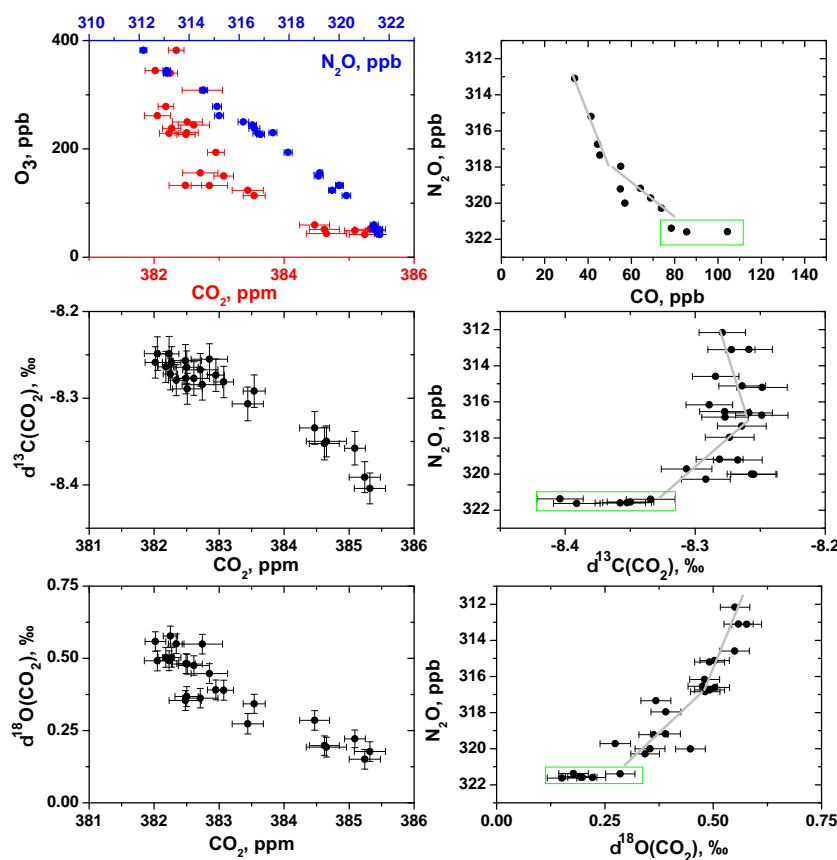
Fig. 5. Flight Frankfurt-Denver-Frankfurt (17–18 December 2007, latitudes 41 to 63° N) crossing the tropopause and demonstrating anti-correlations between O_3, CO and GHG data. The N_2O vs. CO_2 isotope data demonstrate the same compact curvilinear mixing relationship (due to UT/LMS mixing) as typically recorded by O_3 and CO. The CO_2 isotope data plotted vs. CO_2 give linear mixing trends. The correlation between isotope data and stratospheric tracers (N_2O and O_3) is observed for majority of flights that crossed the UT/LMS mixing. Data in the green boxes show UT samples.

4.1.2 General picture of UT/LMS mixing

As CARIBIC-2 covered different flight routes (Fig. 1a, b), we can conclude that CARIBIC has recorded rather general features of UT/LMS mixing in large parts of the NH. To demonstrate a more general picture of CO_2 isotope distribution in the UT/LMS region and similarity of the stratospheric component over different seasons (note, data coverage for some seasons is limited), we plot the data of all CARIBIC flights crossing the UT/LMS (Fig. 7a, b). On this plot we separate data for latitudes > 35° N affected by UT/LMS mixing and latitudes < 35° N which are not affected directly.

Triangle-shaped mixing areas observed for CO_2, $\delta^{13}C(CO_2)$ and $\delta^{18}O(CO_2)$ are formed by seasonally variable signals of UT air masses (Fig. 6). The variability in CO_2 and $\delta^{13}C(CO_2)$ demonstrated by CARIBIC-2 (high-resolution) is larger than that of CARIBIC-1, whereas the general relationships are very similar, except for $\delta^{18}O(CO_2)$ (negative shifts due to exchange in canisters). This agreement exists despite of different flight routes and different

years of observation. The largest variability of CO_2 and isotope signals is within a narrow range of (high) N_2O values (Fig. 7a, b) which corresponds to tropospheric air masses. This is due to both seasonal variations of the signals of UT air masses (Fig. 6) and different degrees of mixing of air masses affected by sources and sinks and background air masses as discussed below.

Towards the stratospheric end member (low N_2O), the variability in all signals diminishes, apparently indicating a single end member mixing ratio (Fig. 7a, b). (All data are de-trended to 1 January 2007). This reflects CO_2 signatures of ascending tropical air (examples are KUM and MLO, Fig. 9) that enters the stratosphere and returns at NH mid-latitudes with some $\delta^{18}O(CO_2)$ modifications. In fact, the back-flux of stratospheric air into the UT does not constitute a single component because it consists of a mixture of air masses having had different stratospheric residence times (age distribution) (Appenzeller et al., 1996; Hall et al., 1999; Andrews et al., 2001; Engel et al., 2009) with a tailing towards older stratospheric air. The stratospheric circulation also attenuates the
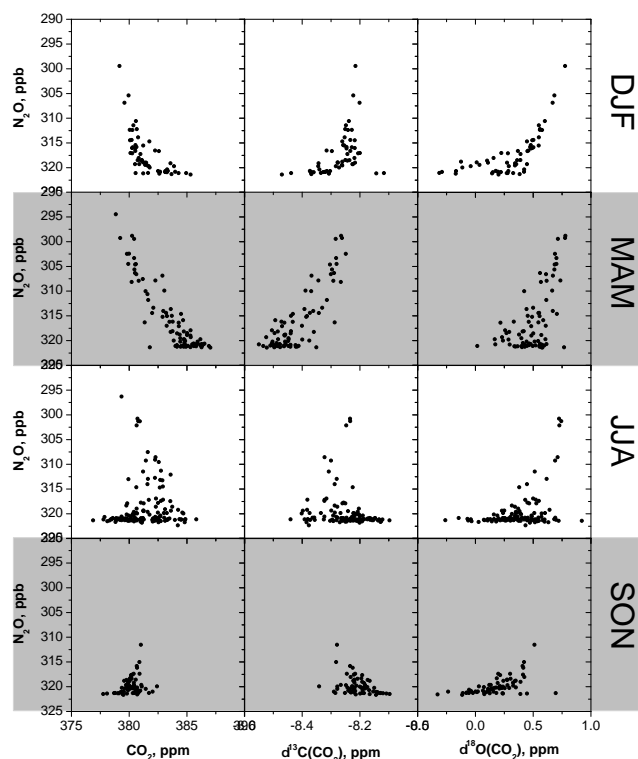
Fig. 6. CARIBIC-2 CO_2 isotope data separated into 4 different seasons and plotted vs. the stratospheric tracer N_2O. Plotted are latitudes above 35° N where UT/LMS mixing takes place. Seasonal variability of UT/LMS trends observed is governed mostly by variability in the UT air.

CO_2 seasonal cycle of ascending air by mixing during transport (Andrews et al., 2001; Strahan et al., 1998). The mean of the age distribution can be approximated by an apparent age, which is defined by decreases of tracers (such as N_2O, CO_2 and SF_6) vs. the signals measured in tropospheric air. The highest apparent SF_6 age for stratospheric samples of CARIBIC-1 is up to 2 years (Assonov, unpublished data). Given that the lowest N_2O values for CARIBIC-2 (Fig. 7b) are about the same as for CARIBIC-1 (Fig. 7a), the apparent ages are to be the same.

The stratospheric flux at mid latitudes is first transported to an intermediate reservoir, namely the LMS as recognized by using CO and O_3 correlations (e.g. Zahn et al., 2004b; Hoor et al., 2004; Pan et al., 2004). This mixing reservoir has a variable ventilation regime, with contributions of stratospheric air, UT air and tropical air masses and exhibits seasonality. There are numerous studies concerning the LMS ventilation (e.g. Zahn et al., 2004a; Hoor et al., 2005; Pan et al., 2000; Stohl et al., 2003). The range of N_2O between 295 and 320 ppb (Fig. 7a, b) clearly reflects this complex mixing; the variability is indeed visible for different seasons (Fig. 6).

Next we consider the $\delta^{18}O(CO_2)$ data. Whereas CO_2 and $\delta^{13}C(CO_2)$ are inert tracers in the stratosphere, $\delta^{17}O(CO_2)$ and $\delta^{18}O(CO_2)$ are not. CO_2 does exchange oxygen isotopes

with O_3 due to photochemical interaction via CO_3, which results from excited $O(^1D)$ radicals reacting with CO_2. The isotopic changes are more clearly correlated with N_2O compared to O_3, the linear trend is valid for N_2O down to 150 ppb (Boering et al., 2004). Although the $^{17}O(CO_2)$ increase is closely coupled with $^{18}O(CO_2)$ (Lämmerzahl et al., 2002), $\Delta^{17}O(CO_2)$ is more robust to analytical artifacts and thus better documented. Therefore, to estimate the stratospheric trend (Fig. 7a, b, lower plots), we first use the $\Delta^{17}O(CO_2)$-N_2O trend (Boering et al., 2004), and subsequently the $\Delta^{17}O(CO_2)/\Delta^{18}O(CO_2)$-ratio of 1.7 (Lämmerzahl et al., 2002). The $\delta^{18}O$-N_2O ratio thus constructed characterizes the trend slope towards low N_2O, taken as 150 ppb.

For fitting CARIBIC-2 observations, the starting point of the stratospheric $\delta^{18}O$-trend was selected to fit CARIBIC-2 observations, being +0.5‰. Overall the CARIBIC-2 data fit the estimated trend well (Fig. 7a, b), with negative deviations being expected due to mixing of air masses having been in contact with land surface. Given that our calibration agrees with NOAA-ESRL (agreement with NIST RMs and NARCIS CO_2 was demonstrated for CARIBIC-1 and CARIBIC-2 (Assonov et al., 2009a, 2009b) whereas consinstency in $\delta^{18}O$ calibration at NOAA-ESRL with other laboratories has been achieved only recently, when NOAA–ESRL corrected their data (White and Vaughn, 2009), the value of +0.5‰ corresponds to a significant contribution of equatorial/tropical air transported to the LMS mixing reservoir (the annual mean in NH tropics, e.g. at MLO over 2001 to 2007 gives +0.49‰). The tropical air contributes to the LMS region by air entering the stratosphere where it resides and certain signatures are modified which trace the age (also leading to ^{18}O modifications). The (direct) contribution of tropical air to the LMS mixing reservoir via complicated transport is discussed by START group members (e.g. Pan et al., 2009) and would correspond to data points being close to the ^{18}O-trend.

The low latitude samples presumably containing a contribution of SH tropical air (which bears more $\delta^{18}O(CO_2)$ higher than +0.5‰ , see Fig. 13a) form a cluster with $N_2O > 320.0$ ppm and $\delta^{18}O(CO_2)$ higher than +0.5‰ (Fig. 7a, b, lowest plots). (No other known process can bring $\delta^{18}O$ to higher values and preserve high N_2O as typical for the troposphere; contribution of SH air is the only explanation.) Besides high $\delta^{18}O(CO_2)$, the free troposphere air masses influenced by SH air have lower CO_2 and higher $\delta^{13}C(CO_2)$; however, by using CO_2 and $\delta^{13}C(CO_2)$, one cannot unambiguously recognize the SH influenced samples, only $\delta^{18}O(CO_2)$ gives clear a indication (ranges of CO_2 and $\delta^{13}C(CO_2)$ in the equatorial zones of the SH and NH are similar, whereas $\delta^{18}O(CO_2)$ has a clear SH-NH gradient). Contribution of SH tropical air to the UT/LMS mixing region in the NH can be excluded on meteorological grounds, and indeed there are only a few positive deviations above the $\delta^{18}O(CO_2)$ trend given by the line on Fig. 7b (lower plot). The same is demonstrated by CARIBIC-1 showing however more positive deviations vs. the $\delta^{18}O(CO_2)$ stratospheric

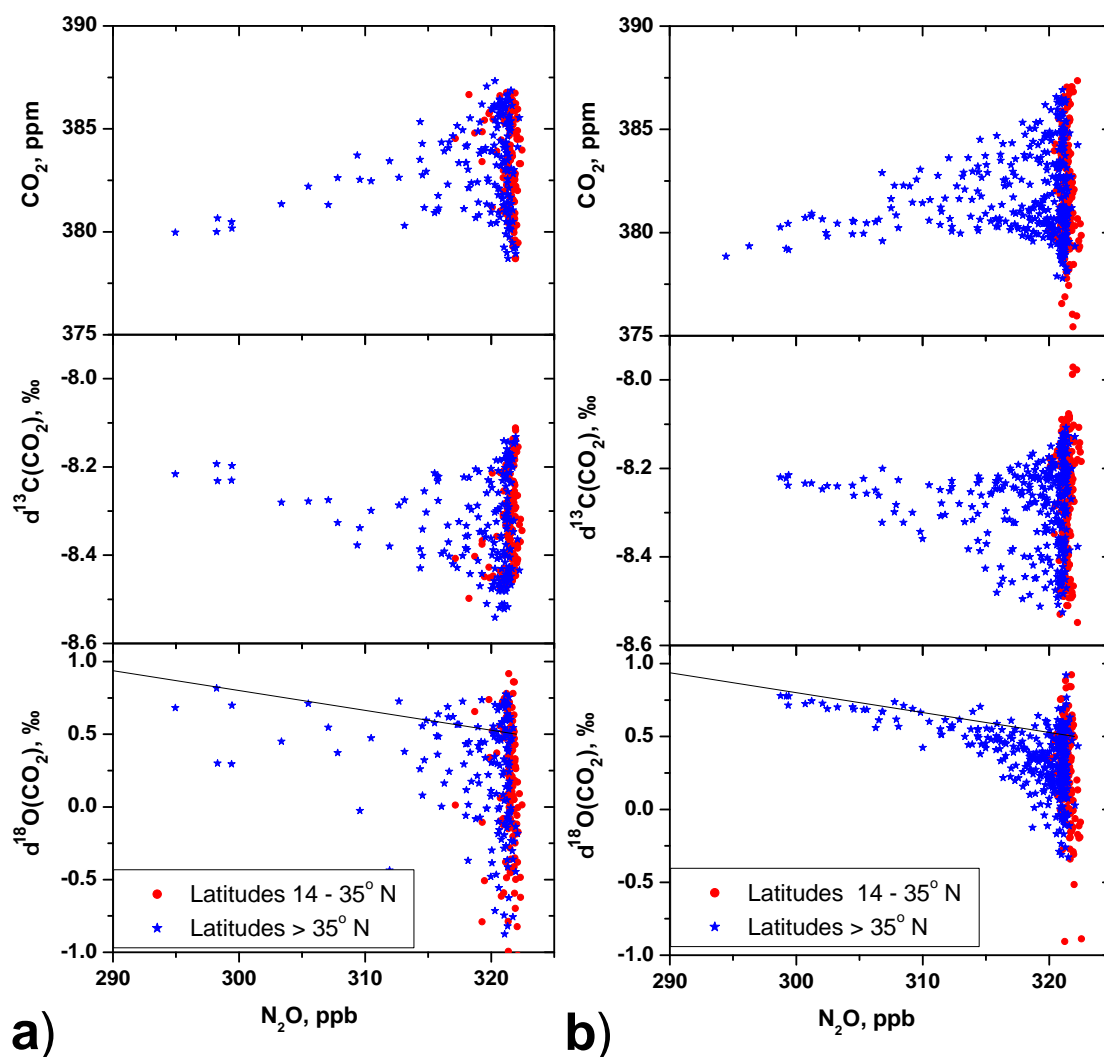**Fig. 7.** The UT/LMS mixing trends for CARIBIC-1 **(a)** and CARIBIC-2 **(b)**. For CARIBIC-2 the trends are visible both in CO_2, $\delta^{13}C(CO_2)$ and in $\delta^{18}O(CO_2)$. The CARIBIC-1 $\delta^{18}O(CO_2)$ data are qualitative only. UT/LMS mixing trends form triangle-shaped areas; this mixing affects latitudes above 35° N only. The trend line for $\delta^{18}O(CO_2)$ is evaluated based on the data for stratospheric CO_2, see text.

trend (note that positive values of CARIBIC-1 are reliable, Assonov et al., 2009b). These positive deviations are likely due to much lower sampling resolution during CARIBIC-1 so that very distinct air masses (SH-affected and LMS-affected) could have been sampled together.

CARIBIC-2 demonstrates numerous deviations below the estimated ^{18}O-trend, thus forming the mixing triangle. There is a third component (or components), characterized by high N_2O combined with $\delta^{18}O(CO_2)$ values below +0.5‰, with variable, mostly low CO_2. The largest number of samples (highest density of all the triangle areas) appears to have $\delta^{18}O(CO_2) = 0.25$‰ and low CO_2 with $\delta^{13}C(CO_2)$ values close to its highest values, around −8.2‰ on the de-trended scale (Fig. 7a, b). At a first glance this may be interpreted as air masses affected by the photosynthetic sink and having being in contact with continental surfaces, which results in lower $\delta^{18}O(CO_2)$. As candidates of transport we

can list fast uplifted (up to 15 km altitude) plumes even crossing the tropopause (e.g. Rhee et al., 2005) as well as isentropic mixing/transport of UT air masses into the LMS (Zahn et al., 2004a) .

Clearly, the new $\delta^{13}C(CO_2)$ and $\delta^{18}O(CO_2)$ data appear to reflect air mixing in the free troposphere and UT/LMS region in a similar way as other tracers such as CO_2, N_2O and SF_6 do. The CO_2 isotope signals in the UT/LMS mixing region resemble signals of tropical air that entered the stratosphere about 2 years prior, accompanied by systematic modifications of $\delta^{18}O(CO_2)$. $\delta^{18}O(CO_2)$ appears to be principally a (new) tracer different from other long lived chemical tracers (such as CO_2, N_2O, SF_6) and also different from $\delta^{13}C(CO_2)$. In the boundary layer $\delta^{18}O(CO_2)$ has a seasonality, a clear latitudinal gradient and SH-NH gradient, and a gradient with lower values over continental interiors (see below). Absent, however is a temporal trend. Therefore, the

distribution of $\delta^{18}O(CO_2)$ in the UT/LMS region can be used as independent information to validate descriptions of global transport and UT/LMS mixing, as well as inter-hemispheric transport in models. Presently the $^{18}O(CO_2)$ "back flux" from the stratosphere is cited as one important unknown in models (Ciais et al., 2005), although proper flux description as well as isotope photochemistry in global circulation models certainly should be able to address this issue. The new data set provides a means by which one can validate future models.

Finally we note that these systematic features illustrate the successful use of N_2O as a linear tracer of UT/LMS mixing for CO_2, $\delta^{13}C(CO_2)$ and $\delta^{18}O(CO_2)$. Similar plots using the O_3 excess relative to the chemical tropopause level (not shown) show more scatter. N_2O mixing trends (on the de-trended data scale) could be translated into mixing proportions of UT and LMS air (if most enriched stratospheric air is defined by a certain N_2O mixing ratio). This feature may be particular useful to describe other chemical tracers in the UT/LMS region.

4.2 Variability in CO_2 and $\delta^{13}C(CO_2)$ for tropospheric air masses

4.2.1 Latitudinal distribution

For the analysis of tropospheric CO_2 we use the CARIBIC-2 data set (latitudes between 14 and 55° N) because sampling is at a higher resolution, the data are more regular compared to CARIBIC-1, and high quality $\delta^{18}O(CO_2)$ are available for all samples. LMS-influenced air masses have been filtered out using the N_2O data.

The de-trended CO_2 data demonstrate no gradient over the latitude range 14 to 55° N (Fig. 8). Such was also noticed by analyses of gradients of CO_2 seasonality over NH latitudes (10 to 50° N, binned in 10° latitudinal bands) (Schuck et al., 2009). Conversely, at the surface significant gradients are caused by especially the large vegetation cover at mid to high latitudes in NH, also resulting in pole-wards increased seasonality (see also "carpet" plots by NOAA, http://www.esrl.noaa.gov/gmd/Photo_Gallery/GMD_Figures/ccgg_figures/). At altitude however, the outflow of the summer monsoon can play a role (Schuck et al., 2010), be it with a restricted geographical footprint.

Tropospheric $\delta^{13}C(CO_2)$ does not demonstrate a latitudinal gradient, which is expected because of the lack of a clear gradient in CO_2. This is again in contrast to gradients for surface stations in the NH representing background (well-mixed troposphere) boundary layer air (see plots by NOAA, http://www.esrl.noaa.gov/gmd/Photo_Gallery/GMD_Figures/ccgg_figures/). However, the limited number of isotope data we have precludes us making a detailed analysis as done for the CO_2 latitudinal gradient (Schuck et al., 2009). $\delta^{18}O(CO_2)$ does not show a gradient, meaning that influx of the photochemically driven modifica-

tion of CO_2 at mid-latitudes is diluted and too small to have an effect for purely UT air masses. (Note that LMS air may penetrate deeply in the troposphere as stratospheric intrusions and filaments (e.g. Cooper et al., 2004; Hocking et al., 2007; Stohl et al., 2000), such air masses were filtered out by N_2O. Here we do not aim to evaluate the total UT/LMS budget). Some lower $\delta^{18}O(CO_2)$ values at 20 to 30° N and, and to a lesser degree at around 50° N indicate fresh plumes that had undergone surface contact in summer (discussed below). A few elevated values for both $\delta^{13}C(CO_2)$ and $\delta^{18}O(CO_2)$ in the SH and close to the equator can be understood as SH-affected air masses, as the CO_2 cycle in the SH differs from that in the NH with high $\delta^{18}O(CO_2)$ being typical for SH air. The CARIBIC-1 data for the SH are also given in Fig. 8 to exemplify typically high SH $\delta^{18}O(CO_2)$ values.

Concerning N_2O the situation is different as N_2O has distinctly lower mixing ratios at mid- and high NH latitudes, which is clearly due to the influx of air from the LMS having lower N_2O mixing ratios (discussed in Sect. 4.2.2). In contrast to CO_2, N_2O seasonality is small and observed variations are mostly due to different air masses mixing, implying that this small gradient is real. Some positive deviations above the main N_2O cluster are due to fresh plumes, whereas negative deviations may indicate the presence of LMS-influenced samples. As stratospheric back flux does take place at these latitudes, such air masses do play a role in a total balance.

Methane (not shown) has a more or less uniform distribution, with high values at about 20 to 30° N due to monsoon plumes (Schuck et al., 2010). The SF_6 data (not shown) show some scatter due to inhomogeneous distribution of sources located in the NH.

Next we revisit the latitudinal distribution of CO_2 (Fig. 8). To understand the latitudinal distribution of the CONTRAIL aircraft CO_2 data obtained at similar flight altitudes, Miyazaki et al. (2008, 2009) applied a global atmospheric transport model. They concluded: "In the NH subtropical upper troposphere, the formation of the latitudinal CO_2 gradient is mostly attributable to the upward and poleward (adiabatic) transports of CO_2..." Based on their model results, the CO_2 concentration gradient at flight altitudes of 300 to 200 hPa is very limited or, in some months negligible. That agrees with the similarity of the range of CO_2 and isotope signals over the corresponding NH latitudes observed by CARIBIC (Fig. 8).

The strongest gradient in the CO_2 latitudinal distribution at flight altitudes appears in summer, at latitudes 45 to 75° N (Fig. 5 in Miyazaki et al., 2008 and also Fig. 3 in Miyazaki et al., 2009). Here lower CO_2 is expected due to uplift of strongly depleted continental air in summer. Though the model of Miyazaki et al. (2008, 2009) does not include the stratospheric flux at mid-latitudes, the effect on concentrations (not directly in UT/LMS structures) cannot be large, about 2% of the maximal LMS/UT variability (see Sect. 4.2.2), which corresponds to up to 0.2 ppm. The model
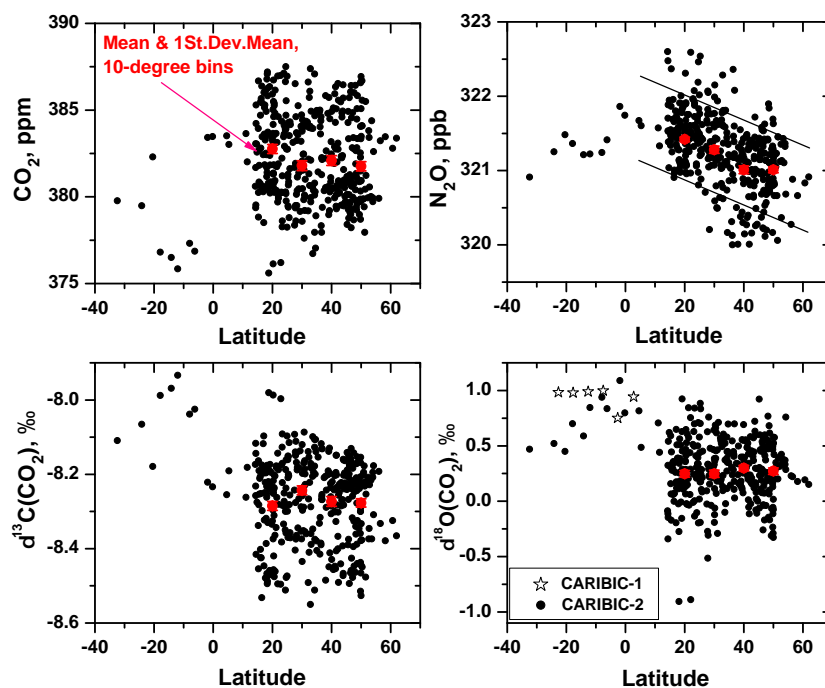
Fig. 8. Latitudinal distributions of CO_2, N_2O and isotope data for CARIBIC-2, flights from April 2007 to March 2009 (de-trended data). Only tropospheric samples from CARIBIC-2 (separated by $N_2O > 320.0$ ppb) and tropospheric $\delta^{18}O(CO_2)$ values of CARIBIC-1 in the SH are shown. Shown in red are Mean values in 10-degree bands, the error bars (close to symbol size) correspond to 1 Std. Dev. of the Mean. Data from CARIBIC-1 for SH air samples are shown for comparison.

results by Shia et al. (2006) show that cross-tropopause exchange is pronounced in certain seasons, but the results do not allow evaluating this contribution correctly. A recent study by Boenisch et al. (2008) aimed to model CO_2 and SF_6 in the extratropical UT/LMS, including STE flux, has demonstrated little gradient at the CARIBIC flight altitudes in the NH latitudes (14 to 55° N), also with an increased gradient in summer.

Recapitulating, pertinent features of the latitudinal distributions are: (i) the absence of gradients in CO_2, $\delta^{13}C(CO_2)$ and $\delta^{18}O(CO_2)$ over latitudes of 14 and 55° N. This is in contrast to the clear latitudinal gradient demonstrated by the NOAA NH surface stations accompanied by increased seasonality (see Fig. 13a, see also surface plots by NOAA, http://www.esrl.noaa.gov/gmd/Photo_Gallery/GM_Figures/ccgg_figures/); (ii) the gradient for N_2O, with high latitude values lower by about 0.5 ppb. These features appear to be in agreement with results of simplified transport models, though stratospheric back flux, UT/LMS mixing structures and isotope distribution are not modeled yet explicitly.

4.2.2 Effect of LMS on the CO_2 isotopic composition in the troposphere

The next issue to address is the effect of the stratosphere-troposphere flux on tropospheric air masses. It has been shown (Nevison et al., 2004, 2007) that the stratospheric influence in the NH significantly contributes to seasonal and inter-annual variations of N_2O and CFCs with long lifetimes having a strong stratospheric sink. These conclusions are based on surface data, thus an effect at flight altitudes is certainly expected. Although we do not intend to evaluate the total N_2O balance in the UT/LMS, one can give some estimation for the dilution brought about by the LMS influx. The N_2O latitudinal gradient (Fig. 8), namely lower N_2O at high NH latitudes, implies a contribution of diluted stratospheric air to UT air. Note that in Fig. 8 LMS air penetrating deeply in the troposphere (e.g. Cooper et al., 2004; Hocking et al., 2007; Stohl et al., 2000) as stratospheric intrusions and mixing filaments was filtered out by N_2O. We estimate this stratospheric contribution to UT air to be about 2% (latitude gradient of 0.5 ppb (Fig. 8) and N_2O range in LMS of 25 ppb (Fig. 7a, b).

By using the range of CO_2 signals observed over the UT/LMS mixing regime (Fig. 7a, b), the above estimate may be translated for the CO_2 isotope budget. The 2% influence means up to 0.01‰ of unresolved shifts in $\delta^{18}O(CO_2)$, which is well below analytical uncertainty. The effect on $\delta^{13}C(CO_2)$ is even lower, within 0.005‰, and cannot be resolved. Because we have no ^{17}O determination for CO_2, the unavoidable $\delta^{13}C(CO_2)$ analytical artifact/bias arising from stratospheric $^{17}O(CO_2)$ enrichment is about 0.04‰ for the most enriched samples (N_2O about 295 ppb) and is diluted to merely 0.001‰ for the 2% influenced UT-samples. Though

these estimations are crude, they show that the stratosphere back flux at high latitudes has negligible effects on ^{13}C and ^{18}O isotope signals in purely tropospheric air masses.

4.2.3 Comparison of tropospheric CO_2 isotope data with those from tropical NOAA stations

Figure 9 gives the seasonal cycles for free and upper tropospheric CO_2, $\delta^{13}C(CO_2)$ and $\delta^{18}O(CO_2)$ as time series with the CARIBIC data (not separated in latitude bands). CARIBIC CO_2 and $\delta^{13}C(CO_2)$ data indeed agree well with those from the selected representative stations in the NH tropics (MLO and KUM) and capture the amplitudes and the seasonality. This agrees with the uplift and poleward transport of tropical NH air (see above). NOAA stations located at higher latitudes and/or on continents show much larger seasonal variability (MHD is shown as example). Though a certain phase shift between CO_2 background/marine boundary layer data from selected stations and signals in the troposphere at the flight altitude can be expected, these aspects are not addressed in this manuscript.

CARIBIC-1 and specifically CARIBIC-2 demonstrate a larger spread of values than results from tropical stations. There may be two separate reasons. For the stations, besides being representative for more homogeneous air masses over the Pacific, monthly mean values are given. The high altitude air probed by CARIBIC does not demonstrate the strong seasonal amplitudes typical for the NH stations directly affected by continental air masses. Even Mace Head (Fig. 9), which has a limited direct impact of continental air masses compared to truly continental NH stations, demonstrates a much larger seasonal amplitude than CARIBIC.

Regardless of the fact that $\delta^{18}O(CO_2)$ is governed by additional processes compared to CO_2 and $\delta^{13}C(CO_2)$, the similarity between CO_2 and $\delta^{13}C(CO_2)$ from CARIBIC and tropical stations implies the same to be expected for $\delta^{18}O(CO_2)$. The CARIBIC-2 $\delta^{18}O(CO_2)$ values mostly agree with those from tropical marine background stations, although some systematic, mostly negative, deviations occur (Fig. 9), chiefly at latitudes of 14 to 30° N (Fig. 8). The deviations in autumn-2008 mainly correspond to monsoon outflow crossed during flights to India. Negative deviations arise from air masses that had been in contact with the surface of continents where intensive ^{18}O exchange with soil and leaf water takes place (Ciais et al., 1997). Such CARIBIC-2 signals are similar to (but more positive than) the data of Mace Head (Fig. 9), a station affected both by marine and continental air. Positive $\delta^{18}O(CO_2)$ values (years 2008 and 2009) of up to 1.0‰ correspond to samples containing SH air which bears more positive $\delta^{18}O(CO_2)$ values (see also Fig. 13a) due to the much smaller land cover. Positive values were also observed by CARIBIC-1 close to the equator and in the SH (Fig. 8).

Thus, comparison of CARIBIC data and the data of NOAA stations in NH tropics agrees with the uplift and pole-

ward transport of tropical air (which forms major features of isotope signals in the troposphere), with significant contribution of plumes.

4.2.4 Carbon cycle and isotope signals

To better understand signals observed by CARIBIC, we briefly summarize the carbon cycle. In the troposphere CO_2 concentration and $\delta^{13}C(CO_2)$ reflect the variability, both in time and space, of CO_2 sources and sinks (respiration, photosynthesis, ocean uptake, fossil fuel and biomass burning). As source and sink processes cause isotope fractionation, variations in CO_2 and $\delta^{13}C(CO_2)$ are closely linked and largely in anti-phase. Photosynthesis produces biomass depleted in ^{13}C with remaining air CO_2 becoming enriched. The isotope fractionation varies between C3, C4 and CAM plants and also depends on water availability (e.g. Bowling et al., 2008).

One can presume that respiration and combustion of fossil fuel and biomass accumulated by photosynthesis will tend to bring air $\delta^{13}C(CO_2)$ back to initial values, opposite to the photosynthesis fractionation. This is only partly true because of a disequilibrium effect – recently formed biomass is linked (by overall photosynthesis fractionation) to modern air $\delta^{13}C(CO_2)$ (around −8.3‰), whereas part of respiration and all combustion releases carbon accumulated in the past when $\delta^{13}C(CO_2)$ was heavier by up to about 2‰ (Francey et al., 1999).

Anthropogenic effects on the CO_2 cycle include fossil fuel burning, increased biomass burning, change of land use, deforestation, erosion, cement production etc. Fossil fuel carbon is characterized by negative $\delta^{13}C(CO_2)$, e.g. around −24‰ for coal, oil from −30 to −26‰, combustion of natural gas mix (biogenic and thermogenic methane) of about −44‰ (e.g. Ciais et al. (1995) and references therein). On average fossil fuel has a $\delta^{13}C(CO_2)$ value of about −28‰, being close to an overall biomass signature.

The gross ocean fluxes exceed the net uptake many times. Ocean uptake has a disequilibrium effect of the same nature as outlined above for photosynthesis – the dissolved CO_2 pool has been in equilibrium with the atmosphere for a long time, when atmospheric $\delta^{13}C(CO_2)$ was higher. Thus the exchange back-flux from the ocean returns CO_2 with $\delta^{13}C(CO_2)$ values higher than the value of the modern CO_2 uptake (e.g. Quay et al., 2003).

The important CO_2 sources and sinks of different $\delta^{13}C(CO_2)$ signatures can be traced using Keeling plots, which are based on the assumption of the admixture of air with CO_2 affected by source and sink processes (accompanied by isotope fractionation) to background air (e.g. Pataki et al., 2003; Miller et al., 2003). The Keeling plots for the remote stations MLO and KUM give the $\delta^{13}C(CO_2)$ intercepts of −14.2 and −14.0‰ (Sect. 3.2), that corresponds to the global inter-annual $\delta^{13}C(CO_2)$ trend. Trend lines for other remote stations (not given) give very similar intercepts,
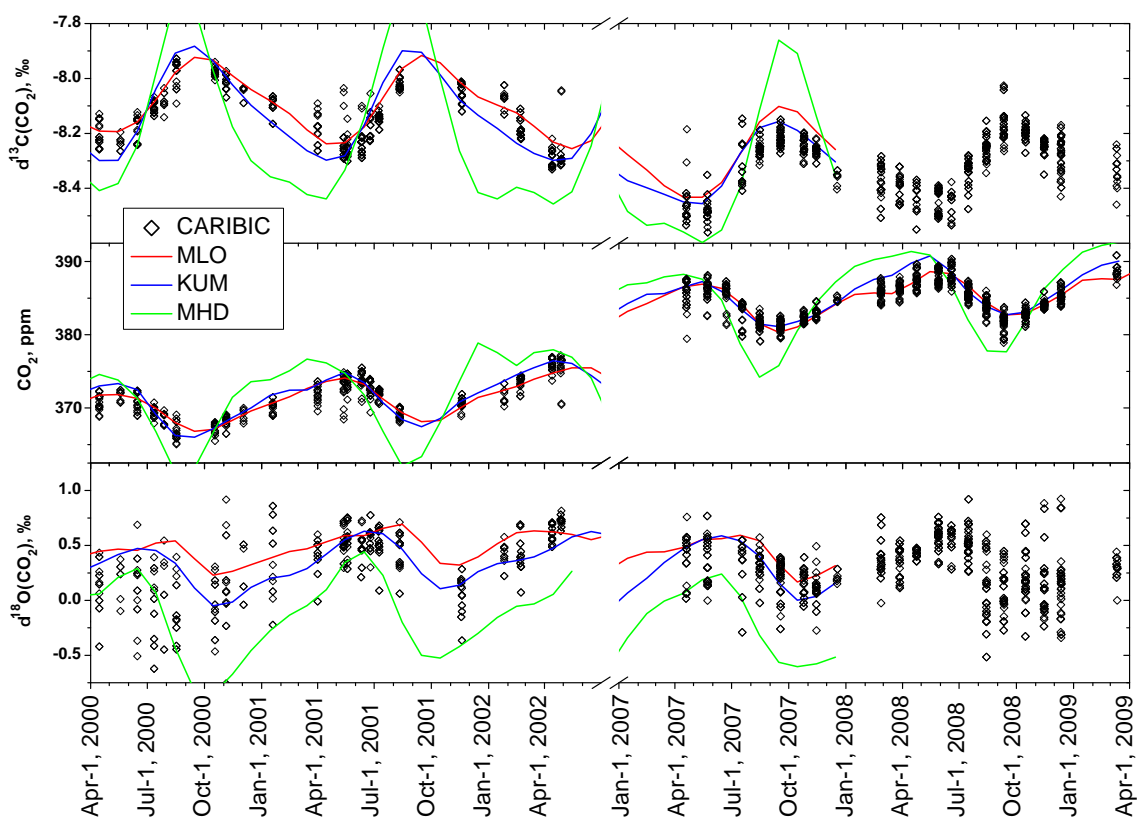
Fig. 9. CO_2, $\delta^{13}C(CO_2)$ and $\delta^{18}O(CO_2)$ data of CARIBIC-1 and CARIBIC-2 (only tropospheric samples, lat. > 14° N) as time series together with data for the stations (MLO, KUM, IZO and MHD, White and Vaughn, 2009). (At the moment of revision, June 2010, NOAA has not released isotope data for 2008.)

e.g. for SPO and BRW at −13.0 and −13.7‰. Though it is not within the scope of this paper to explain these intercepts, we point out that in the absence of the ocean exchange fluxes one would expect the inter-annual trend towards the overall CO_2 sources resulting in CO_2 increase (fossil fuel and biomass burning), the value about −28‰. The agreement between the remote station trend and the CARIBIC-1 vs. CARIBIC-2 trend (see Sect. 4.2.5, also Fig. 11) implies that the intercept of ≈ −14‰ has the global meaning.

4.2.5 Variability in CO_2 and $\delta^{13}C(CO_2)$ of tropospheric air masses

Despite the long distances covered during a single CARIBIC flight (up to 8000 km), good, at times excellent, correlations between $\delta^{13}C(CO_2)$ and CO_2 are evident for many flights (Fig. 10). As an example we show the flight Frankfurt-Toronto-Frankfurt on 17–18 September 2007 with sampling latitudes from 43 to 53° N and 8 day back trajectories reaching from 20 to 70° N (http://www.knmi.nl/samenw/campaign_support/CARIBIC/). After filtering out the LMS contribution using N_2O as described before, GHG and other tracers confirm that we are dealing with pure tropospheric air masses. These tropospheric air masses were nevertheless

of variable origin and history and a number of trace gases, for instance CH_4, showed considerable variability. However, $\delta^{13}C(CO_2)$ correlates extremely well with CO_2 over the 8000 km flight route. The isotope data reveal this correlation for ^{13}C within a total range of merely 0.1‰ thanks to their high precision. This snapshot of a single flight demonstrates large scale similarities of source and sink processes over inter-continental distances.

We emphasize that these compact correlations during single flights reflect source/sink balance for air masses during specific seasons; the intercept of trend lines for such correlations changes during the seasons. Winter and summer correlations demonstrate statistically different intercepts (from −29 to −24‰, plots not shown) due to the variable balance of the most significant sources and sinks of CO_2 in different seasons.

Although a similarity between CO_2 and $\delta^{13}C(CO_2)$ for the CARIBIC time series and data for NH tropical stations (Fig. 9, see above) is observed, the variability of CO_2 and $\delta^{13}C(CO_2)$ during a single flight is large. For remote NOAA stations the variability is mostly seasonal, being observed as time series (the location is fixed and only representative air is sampled). For CARIBIC (moving platform) the variability is
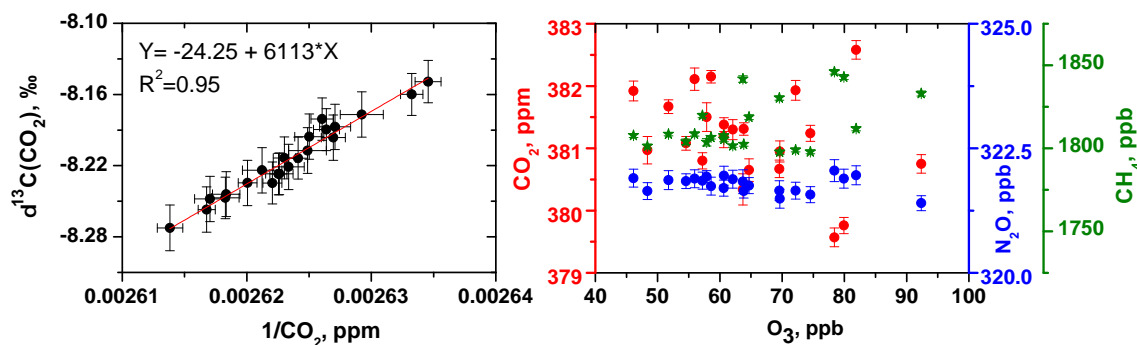
Fig. 10. For a single flight (Frankfurt-Toronto-Frankfurt, September 2007, latitudes 44 to 54° N) an excellent correlation with an extremely narrow range of $\delta^{13}C(CO_2)$ values was observed for tropospheric air masses. The correlation exists despite the influence of different air masses, evidenced by the variability in methane. Right, GHG data for the same flight plotted vs. O_3 demonstrate stable levels of N_2O and variable methane.
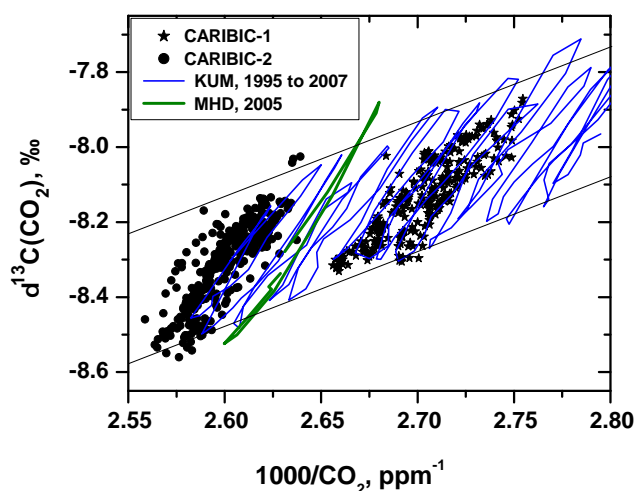

Fig. 11. Keeling plot for CARIBIC-1 and CARIBIC-2 (data not detrended) including data for KUM (1993 to 2007) and MHD (2005). The two enveloping lines correspond to the slope of the KUM interannual trend, and give upper and lower limits of the variability. CARIBIC data agree well with the range demonstrated by the tropical station.

observed both in time and in space, without visible latitudinal gradient in CO_2 (Schuck et al., 2009) and CO_2 isotopes (see above). Thus, along with the seasonal variability, another reason for the variability detected by CARIBIC is the spatial variability (inhomogeneity) in tropospheric air masses at flight altitudes. The fact that variability for high resolution sampling by CARIBIC-2 is much larger than for CARIBIC-1 (see Fig. 9) confirms this.

When $\delta^{13}C(CO_2)$ data (only lat > 14° N) of CARIBIC-1 and CARIBIC-2 are plotted vs. the inverse of the CO_2 mixing ratio, generating a Keeling plot (Fig. 11), nearly all CARIBIC samples are within the amplitude range demonstrated by tropical stations (plotted are data for KUM). CARIBIC-1 and CARIBIC-2 clusters appear to demonstrate

a fine structure, with $\delta^{13}C(CO_2)$ and CO_2 being correlated. Such close correlations between CO_2 and $\delta^{13}C(CO_2)$ are similar to that of Fig. 10. The slope is roughly similar to that of the annual cycle at any NH station with pronounced seasonality, e.g. MHD (Fig. 11). (Seasonal variability of slopes cannot be resolved in Fig. 11). The shift between CARIBIC-1 and CARIBIC-2 clusters agrees with the global trend demonstrated by background stations MLO and KUM; intercept for the stations trend, ≈ -14‰, (Sect. 3.2) mainly characterizes the global CO_2 trend.

Only few CARIBIC data points reach beyond the range of MLO and KUM (Fig. 11). Low values indicate more pronounced effects from respiration, fossil fuel and biomass burning. At times fresh plumes are intersected; for instance the data across biomass burning plumes over China (Lai et al., 2010) demonstrate some correlations between increases in CO and CO_2 and negative shifts in $\delta^{13}C(CO_2)$ (data not plotted). Monsoon plumes were also crossed which were identified by increases in methane and some (negative) $\delta^{18}O(CO_2)$ shifts. High $\delta^{13}C(CO_2)$ values are indicative of a large impact of photosynthesis, also some contribution of SH air cannot be excluded, either. (As CO_2 is a long lived gas, one cannot make a simple mass balance of SH-HN air based e.g. on back-trajectories).

Furthermore, de-trended data of $\delta^{13}C(CO_2)$ and CO_2 show also a good correlation (Fig. 12) and the fit lines for CARIBIC-1 and CARIBIC-2 agree surprisingly well. The de-trending procedure applied has already removed the interannual trend. We interpret the correlated variability in $\delta^{13}C(CO_2)$ and CO_2 as result of mixing of well-mixed background air masses with air masses affected to different degrees by seasonally varying sources and sinks. Accordingly, the agreement between CARIBIC-1 and CARIBIC-2 de-trended data (Fig. 12) indicates that overall balance of all major (global) sources and sinks in NH during the years of CARIBIC-1 and CARIBIC-2 agrees. On the other hand, this agreement implies that the de-trending procedure has not
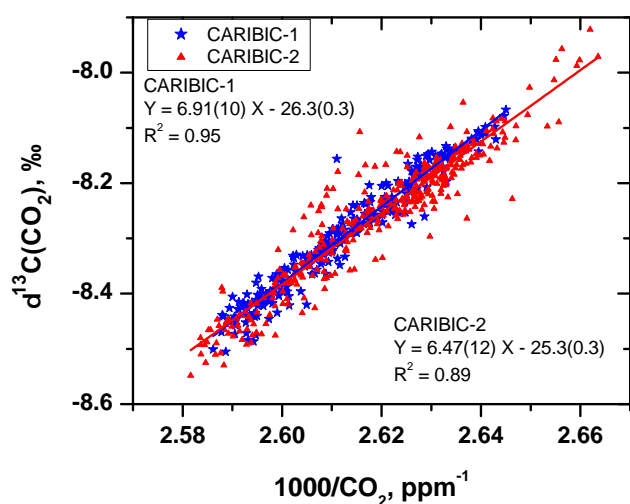
Fig. 12. Keeling plots for $\delta^{13}C(CO_2)$ for de-trended CARIBIC-1 and CARIBIC-2 data showing close agreement (all seasons, data de-trended to 1 January 2007, latitudes > 14° N).

resulted in significant biases.

All in all, we argue that CARIBIC has recorded the main features of a global CO_2 isotope distribution at the flight altitude in the NH. The variability of signals is both due to mixing of different air masses affected by sources and sinks (the matter of atmospheric transport) and the seasonal variability of sources and sinks in the NH. The shift between CARIBIC-1 and CARIBIC-2 data clusters agrees with the global CO_2 trend; de-trended CARIBIC-1 and CARIBIC-2 data agree each other and implies that the budget of major (global) sources and sinks during the years of observation has not changed. The fact that mostly well-mixed air masses have been sampled magnifies the representativeness of the data.

On top of the tropospheric variability there is the variability due to UT/LMS mixing; the latter is well recognized by using stratospheric tracers. We note that the use of isotopes directly reveals the causes for CO_2 variability such as SH air or balance of source and sinks. Without isotopes, one may imply rather a similarity of air masses in the troposphere or data scatter (Schuck et al., 2009), moreover SH air cannot be recognised. However explaining/describing CO_2 and isotope signals of the tropical free troposphere and UT region in detail and making quantitative conclusions, is not trivial and will require advanced coupled biosphere-ocean-atmosphere models; 3-D models are also under development (Cuntz et al., 2003a, b).

4.2.6　Variability in tropospheric $\delta^{18}O(CO_2)$

Of overriding importance for $\delta^{18}O(CO_2)$ and its variations is ^{18}O exchange with water (leaf, soil, and ocean water) via bicarbonate formation. The isotope change depends directly on the $\delta^{18}O(H_2O)$ value while the fractionation constant pos-

sesses a strong temperature dependence (Brenninkmeijer et al., 1983). The variations in $\delta^{18}O(CO_2)$ cannot be detected by the Keeling plot technique, which is based on the assumption that concentration changes are accompanied by isotope fractionation by sources or sinks. Only combustion acts as a source in that sense. However fossil fuel and biomass burning combustion constitute a small flux compared to the gross CO_2 fluxes, whereby CO_2 undergoes ^{18}O exchange. Consequently, $\delta^{18}O(CO_2)$ is a specific tracer of gross CO_2 fluxes. Accurate measurements of $\delta^{18}O(CO_2)$ on a large scale started only years ago (until recently not all NOAA sampling underwent drying, see White and Vaughn, 2009) and not much data interpretation is available (e.g. Cuntz et al., 2003a, b) reported by a 3-D model describing $\delta^{18}O(CO_2)$ on the surface, which they have tested up to 3000 m a.s.l.); understanding ecosystem-atmosphere exchange processes is underway (e.g. Still et al., 2009). We also reiterate that $\delta^{18}O(CO_2)$ is a tracer of air transport and mixing as we demonstrated for the UT/LMS region.

The similarity between $\delta^{13}C(CO_2)$ and CO_2 of CARIBIC and the data of representative stations in the NH tropical boundary layer implies the same similarity to be expected for $\delta^{18}O(CO_2)$. At a first glance (Fig. 9, lowest plot), $\delta^{18}O(CO_2)$ of CARIBIC-1 and CARIBIC-2 demonstrates a scatter, with many negative deviations vs. the NH tropical stations' trends. When plotting $\delta^{18}O(CO_2)$ vs. CO_2, no structure is discernable (Fig. 13b). The year 2008 demonstrates a larger variability than 2007 (plot not given), due to different routes and the Indian summer monsoon.

The NOAA data help in understanding some characteristics of the CARIBIC's $\delta^{18}O(CO_2)$ patterns. First, the amplitude of the $\delta^{18}O(CO_2)$ seasonal cycle systematically increases from the SH to high NH latitudes, whereas the annual means decrease (Fig. 13a). Besides this SH-NH gradient due to the NH land masses, there also are significant gradients across continents. The actual $\delta^{18}O(CO_2)$ values depend on $\delta^{18}O$ of precipitation, temperature, evaporation and evapotranspiration (see e.g. Ciais et al., 1997). The largest $\delta^{18}O(CO_2)$ seasonal cycle in the NH can be best illustrated by the gradient between MLO and Barrow data (Fig. 13a). Thus the CARIBIC $\delta^{18}O(CO_2)$ data appears to reflect very different air masses sampled.

As exchange with water vapor in air is negligible and $\delta^{18}O(CO_2)$ is only affected by dilution with background air, the largest $\delta^{18}O(CO_2)$ variability can be expected in fresh plumes. Indeed, the most prominent negative $\delta^{18}O(CO_2)$ shifts are in autumn 2008 (Fig. 9) for the flights to India which crossed large plumes of surface air (Schuck et al., 2010).

Besides negative deviations from the trend of NH tropical stations, there are some positive deviations. The highest $\delta^{18}O(CO_2)$ values are around +0.9‰ in November-December 2008 at about 20° N (Fig. 9) which are believed to have been due to significant contributions of SH air with high $\delta^{18}O(CO_2)$ values (Fig. 13a). In fact high values (around

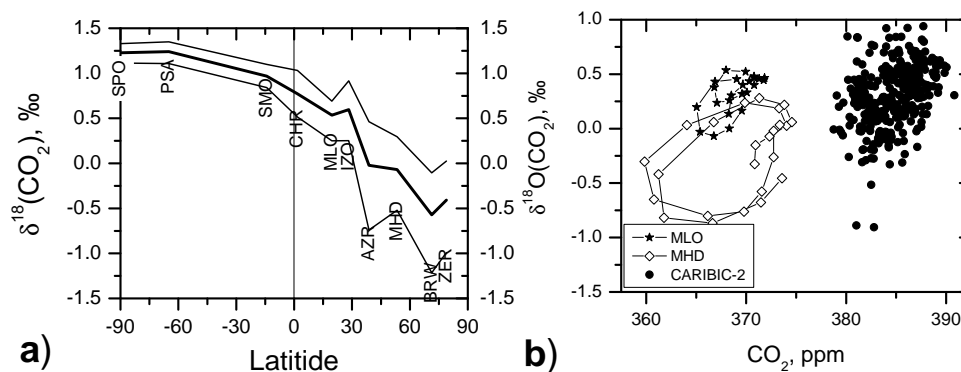**Fig. 13. (a)** Global latitudinal gradient of the $\delta^{18}O(CO_2)$ seasonal cycle, data for NOAA stations (White and Vaughn, 2009). Mean values and the amplitudes, averaged for years 2003 to 2005 are shown. **(b)** The $\delta^{18}O(CO_2)$ seasonal cycle at Mauna Loa and Mace Head, years 1999–2000. The cycle direction is anti-clock wise. CARIBIC-2 data: tropospheric air, latitudes > 14° N.

+ 1.0‰) were also recorded for samples collected close to the equator and in the SH (African flights) by CARIBIC-1 (March 3, 2000) and CARIBIC-2 (March, 2009) (Fig. 8).

4.2.7 Seasonal cycle of $\delta^{13}C(CO_2)$ and CO_2 in the troposphere

Lastly, based on de-trended data, we evaluate the seasonal cycle of $\delta^{13}C(CO_2)$ and CO_2 in the troposphere. CARIBIC-1 and CARIBIC-2 data demonstrate basically the same seasonality and amplitude (Fig. 14a). This agreement implies the data to be really representative for remote background air. Noting that CARIBIC-1 and CARIBIC-2 have different flight routes, that measurements were performed by different sampling and extraction systems, in two different laboratories, with a time lag of 5 years, the agreement gives confidence that representative isotope data of required precision can be obtained.

After filtering out data of fresh plumes (by total H_2O above 2000 ppb and CO above 125 ppb; these levels were selected based on a signal distribution, and only a few data points were removed), the tropospheric data of CARIBIC-2 are in line with the phase and the range of values at the NOAA stations in the NH tropics (Fig. 14b). As discussed above, CARIBIC, being a moving platform, demonstrates higher variability than selected stations where only background air masses are sampled. The variability of tropospheric signals at flight altitudes is due to mixing of air masses affected by sources and sinks with background air; the effect of UT/LMS mixing is limited. CARIBIC-2 data presented using the boxplot (Fig. 14b) can be considered as monthly values of background air in the troposphere at flight altitude. The agreement with data from NOAA NH tropical stations supports uplift and transport of tropical air at flight altitudes being the major driving mechanisms.

4.3 Future use of data, optimal sampling resolution and aspects of analytical errors

Our expectation is that in the future the data will be requested and used in global models. We note that data generation always preceded model developments: although regular CO_2 monitoring began in 1957 (at Mauna Loa, by Keeling), the data use in models started much later that the data became available. Thus, having the opportunity to obtain reliable CO_2 isotope composition by the CARIBIC aircraft platform, we did so in the hope that that data could be useful in global models. Capabilities to analyze CO_2 isotope composition by CONTRAIL are under development; to our knowledge, to-date CONTRAIL has neither presented nor published CO_2 isotope data.

When one intends to obtain representative information on the global CO_2 cycle with limited capabilities, optimizing sampling strategy is crucial. In our case, optimal flight frequency, the distance covered by a single sample, and the sampling frequency all need consideration. On the one hand, sampling at low resolution, similar to that of most models ($2 \times 2°$ grid at best) is logical. High-resolution sampling gives a more detailed picture of mixing effects and structures involved, but the information, given a certain sample capacity, is reduced, meaning that some data extrapolation in models will be required.

Comparing CARIBIC-1 and CARIBIC-2 data in this context is useful. Obviously the high sampling resolution by CARIBIC-2 (15 km of flight distance per sample) with 14 samples per outward and return flight gives a different picture than obtained with the low resolution CARIBIC-1 samples (250 km per sample, 12 samples per flight). This is well illustrated by the UT/LMS mixing trends (Figs. 5, 6 and 7a, b). CARIBIC-2 data clearly demonstrate the compact curvilinear mixing relationship in the UT/LMS region, which is visible both for $\delta^{13}C(CO_2)$ and $\delta^{18}O(CO_2)$, occasionally $\delta^{18}O(CO_2)$ shows even more regular patterns than
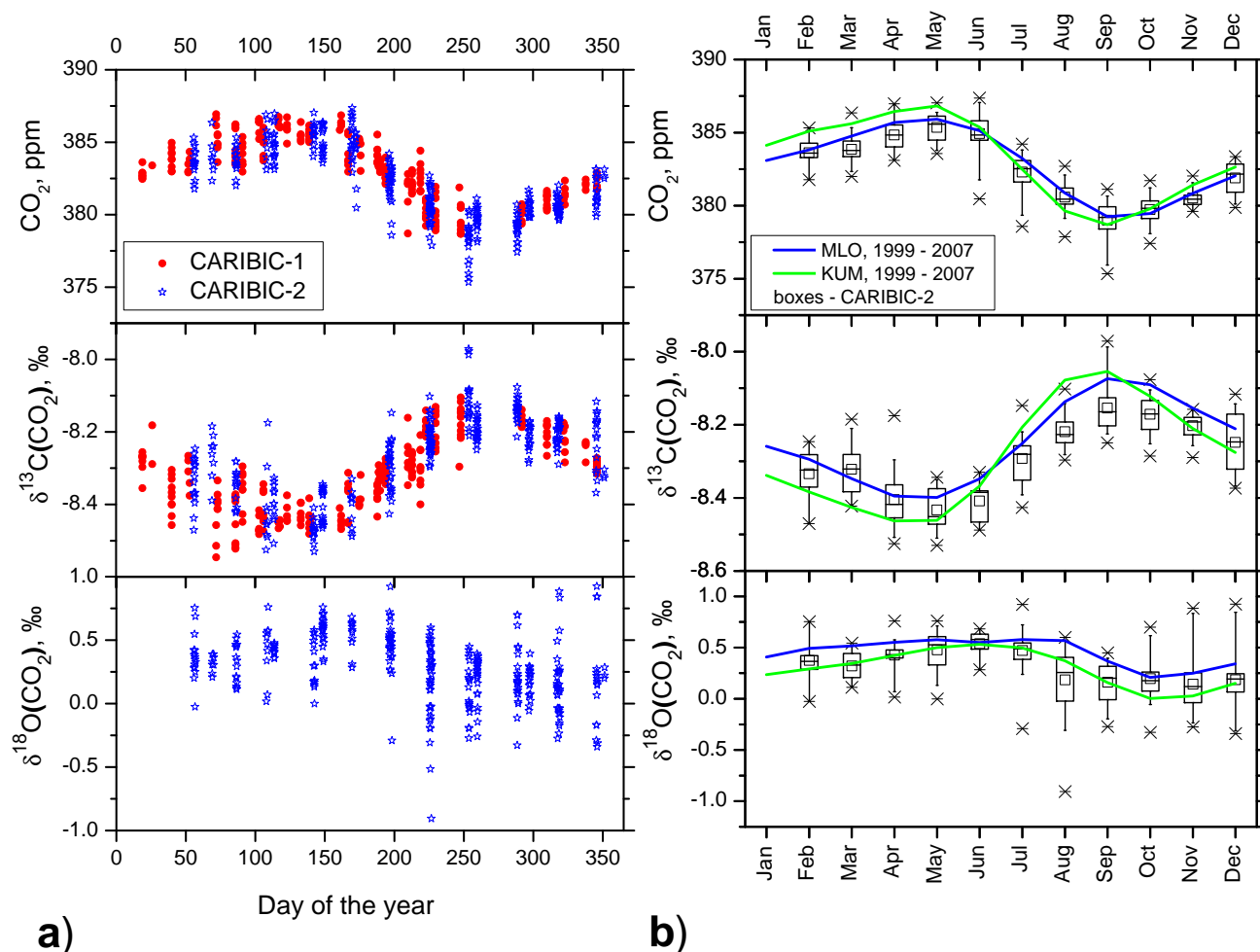
Fig. 14. **(a)** Seasonality for tropospheric air masses detected by CO_2 isotopes; all flights, latitudes > 14° N. Data de-trended to 1 January 2007. **(b)** The 1999 to 2007 averaged monthly mean data for KUM and MLO (de-trended data) and tropospheric CARIBIC-2 data (box-plots). Plumes evidenced by very high water and high CO are filtered out (H_2O > 2000 ppm and CO > 125 ppb). Box ranges are at 25, 50 and 75%, Whiskers are at 5 and 95%, square corresponds to the Median and crosses indicate Min and Max values.

$\delta^{13}C(CO_2)$. In contrast, UT/LMS data from CARIBIC-1 show only linear trends for $\delta^{13}C(CO_2)$ without details or systematic patterns for $\delta^{18}O(CO_2)$. (Some CARIBIC-1 trends are given by Assonov et al., 2007). Low and high resolution sampling ultimately give different data sets. When one aims to study frequent tropopause crossings at mid latitudes, a higher resolution may be preferable.

The data uncertainty needs to be in line with the variability detected, to be considered from the point of future data use. At cruise altitudes, the variability detected in tropospheric air masses (de-trended data) is about 10 ppm for CO_2 and 0.4‰ for $\delta^{13}C(CO_2)$. Given that total combined uncertainty we have reached are respectively 0.2 ppm and 0.02‰ (1-σ values, that is, a 20 ppm variation in the 1.1% ^{13}C in carbon), this translates into 2% and 5% relative variability. This is a rather reasonable balance between signals and errors. The correlations observed between CO_2 and $\delta^{13}C(CO_2)$

(e.g. Fig. 10) imply that at the moment actual analytical errors in CO_2 and $\delta^{13}C(CO_2)$ (at the level of our laboratory performance) are rather well balanced.

We stress that for meaningful use of such data in models, data merging between different laboratories is critical. The only inter-laboratory comparison performed was with MPI-BGC, Jena, during which the discrepancies of −0.04 and −0.06‰ for $\delta^{13}C(CO_2)$ and $\delta^{18}O(CO_2)$ were documented (Assonov et al., 2009a). Although this exceeds the 1-σ errors evaluated by the two laboratories and exceeds the $\delta^{13}C(CO_2)$ compatibility target of merging data from different laboratories (Expert Group Recommendations of 13th_WMO/IAEA_Meeting), inter-laboratory scale discrepancies observed by round robins among other laboratories are, unfortunately, much larger (Levin et al., 2007). Such discrepancies were recognized long time ago (Masarie et al., 2001) as having several potential sources (e.g. Vaughn et al.,

2010); resolving these aspects is beyond the scope of this paper. Importantly, the offset between MPI-BGC and NOAA being documented is limited and stable in time (Levin et al., 2007), permitting the reconstruction of a (possible) offset between the NOAA scale realization and the IRMM and MPI-C scale realization.

All the GHG and isotope data obtained by CARIBIC being presently stored on the CARIBIC data server are available upon request to the project coordinator Carl Brenninkmeijer.

5   Summary and outlook

1. CARIBIC provided unique isotope data sets for the UT/LMS and free tropical troposphere, with about 1 month resolution. CARIBIC-1, with low resolution sampling provided high quality $\delta^{13}C(CO_2)$ data (1999 to April 2002) and $\delta^{18}O(CO_2)$ data (October 2000 and April 2002). CARIBIC-2 (April 2007–March 2009) resulted in precise, accurate and reliable $\delta^{13}C(CO_2)$ and $\delta^{18}O(CO_2)$ data from high-resolution sampling. For all samples extensive supporting GHG, O_3, CO and meteorological data are available.

2. The manuscript presents the first analyses of the CARIBIC data for tracer-tracer correlations, distribution and trends with detailed information for UT/LMS CO_2, $\delta^{13}C(CO_2)$ and $\delta^{18}O(CO_2)$. For the first time it is demonstrated that global-scale variability in air mass origin and GHG signals are reflected by the variability in $\delta^{13}C(CO_2)$ and $\delta^{18}O(CO_2)$. Besides the UT/LMS mixing, such correlations arise from different degrees of mixing of background air with air masses affected by sources and sinks, over the distance up to 8000 km and also over different seasons. The trends and features demonstrated by CARIBIC-2 are found to agree with CARIBIC-1 signals attenuated over long sampling distance.

3. Data de-trending and use of stratospheric tracers is considered. N_2O is discussed to be the most suitable tracer in describing mixing proportions of CO_2 signals in the UT/LMS region. (N_2O can also be successfully applied to other chemical tracers in the UT/LMS region.) By filtering out LMS data (using N_2O as a stratospheric tracer) and data from fresh plumes, CO_2 isotope data tropospheric background air masses were obtained. The data and trends agree well with the data of NOAA stations in the NH tropics. This is in agreement with global atmospheric transport, namely with the uplift and transport of tropical air masses poleward.

4. The $\delta^{18}O(CO_2)$ data reflect well air mixing in the free troposphere and UT/LMS region. $\delta^{18}O(CO_2)$ appears to be a fundamentally different tracer than other long lived chemical tracers (such as CO_2, N_2O, SF_6) as it

has both a seasonality and clear latitudinal gradient, in the absence of a long-term temporal trend. Therefore the distribution of $\delta^{18}O(CO_2)$ in the UT/LMS region can be used as an independent tracer to validate description of global (and also interhemispheric) transport and UT/LMS mixing in models.

5. Climate change will most likely show up in $\delta^{18}O(CO_2)$ data. Although it is a highly complex signal, its link to temperature, humidity, soils and vegetation makes it desirable to monitor $\delta^{18}O(CO_2)$, not only at the surface, but also at altitude, in well mixed air masses. Thereafter the obtained present-day record for the free troposphere and UT/LMS region is an asset to future comparisons.

6. Considering future developments of observations by aircraft, sampling resolution and optimal analytical uncertainty are critical. While high-resolution sampling is extremely valuable to study in detail effects of UT/LMS mixing and inter-hemispheric transport, it may be less applicable when one aims at obtaining representative signals for the remote troposphere on the global scale, for use in models.

7. The data shown are based on a major research effort (made possible by IRMM in Geel, Belgium for CARIBIC-2), that could not be sustained at present but should be taken up again in the not too distant future. An 88 sampling system in CARIBIC-2, to operate in addition to the 28 sample system, has been deployed since early 2010, marking the next challenging step for CO_2 isotope measurements.

Appendix A

Abbreviations

CARIBIC – Civil Aircraft for the Regular Investigation of the atmosphere Based on an Instrument Container, www.caribic-atmospheric.com

GHG – green house gases;

CONTRAIL – Comprehensive Observation Network for TRace gases by AIrLiner, research project by NIES, Japan

LMS – lowermost stratosphere

LS – lower stratosphere

MPI-BGC – Max Planck Institute for Bio-Geochemistry, Jena, DE;

MPI-C – Max Planck Institute for Chemistry, Mainz, DE;

NARCIS – NIES Atmospheric Reverence CO_2 for Isotopic Studies

NH – Northern Hemisphere

NIES – National Institute for Environmental Studies, Japan

NIST – National Institute of Standards and Technology, USA

NOAA – the National Oceanic and Atmospheric Administration, USA

NOAA-ESRL – Earth System Research Laboratory at NOAA, USA

ppb – parts per billion, volumetric

ppm – parts per million, volumetric

RM – reference material

STE – stratosphere-troposphere exchange

SH – Southern Hemisphere

UT – upper troposphere

UT/LMS – upper troposphere-lowermost stratosphere

NOAA stations are given by using the following abbreviations

AZR – Terceira Island, Azores, Portugal, 38.77° N; 27.38° W; 40 m a.s.l.;

KUM – Cape Kumukahi, Hawaii, USA, 19.52° N; 154.82° W; 3 m a.s.l.;

IZO – Tenerife, Canary Islands, Spain, 28.3° N, 16.48° W; 2360 m a.s.l.;

MHD – Mace Head, Ireland, 53.33° N; 9.9° W; 25 m a.s.l.;

MID – Sand Island, Midway, USA, 28.21° N; 177.38° W; 7.7 m a.s.l.;

MLO – Mauna Loa, Hawaii, USA, 19.54° N, 155.58° W; 3397 m a.s.l.

Edited by: J. Kaiser

References

Allison, C. E., Francey, R. J., and Meijer, H. A. J.: Recommendation for the reporting of stable isotope measurements of carbon and oxygen in CO$_2$ gas, IAEA-TECDOC-825, Vienna, IAEA-TECDOC-825, 155–162, 1995.

Allison, C. E. and Francey R. J.: Verifying Southern Hemisphere trends in atmospheric carbon dioxide stable isotopes, J. Geophys. Res.-Atmos, 112, D21304, doi:21310.21029/22006JD007345, 2007.

Andrews, A. E., Boering, K. A., Daube, B. C., Wofsy, S. C., Loewenstein, M., Jost, H., Podolske, J. R., Webster, C. R., Herman, R. L., Scott, D. C., Flesch, G. J., Moyer, E. J., Elkins, J. W., Dutton, G. S., Hurst, D. F., Moore, F. L., Ray, E. A., Romashkin, P. A., and Strahan, S. E.: Mean ages of stratospheric air derived from in situ observations of CO$_2$, CH$_4$, and N$_2$O, J. Geophys. Res.- Atmos., 106, 32295–32314, 2001.

Appenzeller, C., Holton, J. R., and Rosenlof, K. H.: Seasonal variation of mass transport acrossthe tropopause, J. Geophys. Res.-Atmos., 10, 15071–15078, 1996.

Assonov, S., Taylor, P., and Brenninkmeijer, C. A. M.: A system for high-quality CO$_2$ isotope analyses of air samples collected by the CARIBIC Airbus A340-600, Rapid Commun. Mass Sp., 23, 1347–1363, 2009a.

Assonov, S. S. and Brenninkmeijer, C. A. M.: A re-determination of absolute values for ^{17}R$_{VPDB-CO_2}$ and ^{17}R$_{VSMOW}$, Rapid Commun. Mass Sp., 17, 1017–1029, 2003.

Assonov, S. S., Brenninkmeijer, C. A. M., Zahn, A., and Koeppel, C.: CO$_2$ isotopic composition in the upper troposphere: the project CARIBIC, 14th WMO/IAEA Meeting of Experts on Carbon Dioxide Concentration and Related Tracers Measurement Techniques, Helsinki, Finnland, 9–22 September 2007; WMO Tec-Doc No. 1487, WMO/GAW report No. 186, 90–93, available at: http://www.wmo.int/pages/prog/arep/gaw/documents/ GAW_186_TD_No_1487_web.pdf,(last access: September 2010), 2007.

Assonov, S. S., Brenninkmeijer, C. A. M., Koeppel, C., and Röckmann, T.: CO$_2$ isotope analyses using large air samples collected on intercontinental flights by the CARIBIC Boeing 767, Rapid Commun. Mass Sp., 23, 822–830, 2009b.

Bender, M. L., Ho, D. T., Hendricks, M. B., Mika, R., Battle, M. O., Tans, P. P., Conway, T. J., Sturtevant, B., and Cassar, N.: Atmospheric O$_2$/N$_2$ changes, 1993–2002: Implications for the partitioning of fossil fuel CO$_2$ sequestration, Global Biogeochem. Cy., 19, GB4017, doi:10.1029/2004gb002410, 2005.

Bischof, W. and Bolin, B.: Space and time variations of CO$_2$ content of troposphere and lower stratosphere, Tellus 18, 155–159, 1966.

Boenisch, H., Hoor, P., Gurk, C., Feng, W., Chipperfield, M., Engel, A., and Bregman, B.: Model evaluation of CO$_2$ and SF$_6$ in the extratropical UT/LS region, J. Geophys. Res., 113, D06101, doi:10.1029/2007JD008829, 2008.

Boering, K. A., Jackson, T., Hoag, K. J., Cole, A. S., Perri, M. J., Thiemens, M., and Atlas, E.: Observations of the anomalous oxygen isotopic composition of carbon dioxide in the lower stratosphere and the flux of the anomaly to the troposphere, Geophys. Res. Lett., 31, L03109, doi:03110.01029/02003GL018451, 2004.

Bowling, D. R., Pataki, D. E., and Randerson, J. T.: Carbon isotopes in terrestrial ecosystem pools and CO$_2$ fluxes, New Phytol., 178,

24–40, 2008.

Brand, W. A., Assonov, S. S., and Coplen, T. B.: Correction for the ^{17}O interference in $\delta(^{13}C)$ measurements when analyzing CO_2 with stable isotope mass spectrometry (IUPAC Technical Report), Pure Appl. Chem., 82(8), 1719–1733, doi:10.1351/PAC-REP-09-01-05, 2010.

Brenninkmeijer, C. A. M., Kraft, P., and Mook, W. G.: Oxygen isotope fractionation between CO_2 and H_2O, Isot. Geosci., 1, 181–190, 1983.

Brenninkmeijer, C. A. M., Crutzen, P. J., Fischer, H., Gusten, H., Hans, W., Heinrich, G., Heintzenberg, J., Hermann, M., Immelmann, T., Kersting, D., Maiss, M., Nolle, M., Pitscheider, A., Pohlkamp, H., Scharffe, D., Specht, K., and Wiedensohler, A.: CARIBIC – Civil aircraft for global measurement of trace gases and aerosols in the tropopause region, J. Atmos. Ocean. Techn., 16, 1373–1383, 1999.

Brenninkmeijer, C. A. M., Crutzen, P., Boumard, F., Dauer, T., Dix, B., Ebinghaus, R., Filippi, D., Fischer, H., Franke, H., Frieß, U., Heintzenberg, J., Helleis, F., Hermann, M., Kock, H. H., Koeppel, C., Lelieveld, J., Leuenberger, M., Martinsson, B. G., Miemczyk, S., Moret, H. P., Nguyen, H. N., Nyfeler, P., Oram, D., O'Sullivan, D., Penkett, S., Platt, U., Pupek, M., Ramonet, M., Randa, B., Reichelt, M., Rhee, T. S., Rohwer, J., Rosenfeld, K., Scharffe, D., Schlager, H., Schumann, U., Slemr, F., Sprung, D., Stock, P., Thaler, R., Valentino, F., van Velthoven, P., Waibel, A., Wandel, A., Waschitschek, K., Wiedensohler, A., Xueref-Remy, I., Zahn, A., Zech, U., and Ziereis, H.: Civil Aircraft for the regular investigation of the atmosphere based on an instrumented container: The new CARIBIC system, Atmos. Chem. Phys., 7, 4953–4976, doi:10.5194/acp-7-4953-2007, 2007.

Callendar, G. S.: The Artificial Production of Carbon Dioxide and Its Influence on Temperature, Q. J. Roy. Meteorol. Soc., 64, 223–240, 1938.

Ciais, P., Tans, P. P., White, J. W. C., Trolier, M., Francey, R. J., Berry, J. A., Randall, D. R., Sellers, P. J., Collatz, J. G., and Schimel, D. S.: Partitioning of Ocean and Land Uptake of CO_2 as Inferred by $\delta^{13}C$ Measurements from the NOAA Climate Monitoring and Diagnostics Laboratory Global Air Sampling Network, J. Geophys. Res.-Atmos., 100, 5051–5070, 1995.

Ciais, P., Denning, A. S., Tans, P. P., Berry, J. A., Randall, D. A., Collatz, G. J., Sellers, P. J., White, J. W. C., Trolier, M., Meijer, H. A. J., Francey, R. J., Monfray, P., and Heimann, M.: A three-dimensional synthesis study of $\delta^{18}O$ in atmospheric CO_2.1. Surface fluxes., J. Geophys. Res.-Atmos., 102, 5857–5872, 1997.

Ciais, P., Cuntz, M., Scholze, M., Mouillot, F., Peylin, P., and Gitz, V.: Remarks on the use of ^{13}C and ^{18}O isotopes in Atmospheric CO_2 to Quantify biospheric carbon fluxes, in: Stable Isotopes and Biosphere Atmosphere Interactions, Academic Press, San Diego, 235–267, 2005.

Conway, T. J., Lang, P. M., and Masarie, K. A : Atmospheric Carbon Dioxide Dry Air Mole Fractions from the NOAA ESRL Carbon Cycle Cooperative Global Air Sampling Network, 1968–2008, Version: 15 July 2009, Path: ftp://ftp.cmdl.noaa.gov/ccg/co2/flask/event/, 2009.

Cooper, O., Forster, C., Parrish, D., Dunlea, E., Hübler, G., Fehsenfeld, F., Holloway, J., Oltmans, S., Johnson, B., Wimmers, A., and Horowitz, L.: On the life cycle of a stratospheric intrusion and its dispersion into polluted warm conveyor belts, J. Geophys. Res., 109, D23S09, doi:10.1029/2003jd004006, 2004.

Cuntz, M., Ciais, P., Hoffmann, G., Allison, C. E., Francey, R. J., Knorr, W., Tans, P. P., White, J. W. C., and Levin, I: A comprehensive global three-dimensional model of $\delta^{18}O$ in atmospheric CO_2: 2. Mapping the atmospheric signal, J. Geophys. Res.-Atmos., 108(D17), 4528, doi:4510.1029/2002JD003154, 2003a.

Cuntz, M., Ciais, P., Hoffmann, G., Allison, C. E., Francey, R. J., Knorr, W., Tans, P. P., White, J. W. C., and Levin, I.: A comprehensive global three-dimensional model of $\delta^{18}O$ in atmospheric CO_2: 2. Mapping the atmospheric signal, J. Geophys. Res.-Atmos., 108, 4528, doi:4510.1029/2002JD003154, 2003b.

Dlugokencky, E. J., Steele, L. P., Lang, P. M., and Masarie, K. A.: The growth rate and distribution of atmospheric methane, J. Geophys. Res., 99, 17021–17043, 1994.

Engel, A., Mobius, T., Bonisch, H., Schmidt, U., Heinz, R., Levin, I., Atlas, E., Aoki, S., Nakazawa, T., Sugawara, S., Moore, F., Hurst, D., Elkins, J., Schauffler, S., Andrews, A., and Boering, K.: Age of stratospheric air unchanged within uncertainties over the past 30 years, Nat. Geosci., 2, 28–31, 2009.

Expert Group Recommendations of 13th WMO/IAEA Meeting: 13th WMO/IAEA Meeting of Experts on Carbone Dioxide Concentration and Related Tracers Measurement Techniques, Boulder, Colorado, USA, 19–22 September 2005, WMO Tec-Doc No. 1359, WMO/GAW report No. 161, available at: ftp://ftp.wmo.int/Documents/PublicWeb/arep/gaw/gaw168.pdf, (last access: September 2010), 2005.

Francey, R. J., Allison, C. E., Etheridge, D. M., Trudinger, C. M., Enting, I. G., Leuenberger, M., Langenfelds, R. L., Michel, E., and Steele, L. P.: A 1000-year high precision record of $\delta^{13}C$ in atmospheric CO_2, Tellus, 51B, 170–193, 1999.

Hall, T. M., Waugh, D. W., Boering, K. A., and Plumb, R. A.: Evaluation of transport in stratospheric models, J. Geophys. Res.-Atmos., 104, 18815–18839, 1999.

Hegglin, M. I. and Shepherd, T. G.: O_3-N_2O correlations from the Atmospheric Chemistry Experiment: Revisiting a diagnostic of transport and chemistry in the stratosphere, J. Geophys. Res., 112, doi:10.1029/2006jd008281, 2007.

Hocking, W. K., Carey-Smith, T., Tarasick, D. W., Argall, P. S., Strong, K., Rochon, Y., Zawadzki, I., and Taylor, P. A.: Detection of stratospheric ozone intrusions by windprofiler radars, Nature, 450, 281–284, 2007.

Hoor, P., Gurk, C., Brunner, D., Hegglin, M. I., Wernli, H., and Fischer, H.: Seasonality and extent of extratropical TST derived from in-situ CO measurements during SPURT, Atmos. Chem. Phys., 4, 1427–1442, doi:10.5194/acp-4-1427-2004, 2004.

Hoor, P., Fischer, H., and Lelieveld, J.: Tropical and extratropical tropospheric air in the lowermost stratosphere over Europe: A CO-based budget, Geophys. Res. Lett., 32, L07802, doi:07810.01029/02004GL022018, 2005.

Jiang, X., Ku, W. L., Shia, R.-L., Li, Q., Elkins, J. W., Prinn, R. G., and Yung, Y. L.: Seasonal cycle of N_2O: Analysis of data, Global Biogeochem. Cy., 21, doi:10.1029/2006gb002691, 2007.

Keeling, C. D.: The concentration and isotopic abundances of carbon dioxide in rural and marine air, Geochim. Cosmochim. Ac., 24, 277–298, 1961.

Köppe, M., Hermann, M., Brenninkmeijer, C. A. M., Heintzenberg, J., Schlager, H., Schuck, T., Slemr, F., Sprung, D., van Velthoven, P. F. J., Wiedensohler, A., Zahn, A., and Ziereis, H.: Origin of aerosol particles in the mid-latitude and subtropical upper troposphere and lowermost stratosphere from cluster

analysis of CARIBIC data, Atmos. Chem. Phys., 9, 8413–8430, doi:10.5194/acp-9-8413-2009, 2009.

Lai, S. C., Baker, A. K., Schuck, T. J., van Velthoven, P., Oram, D. E., Zahn, A., Hermann, M., Weigelt, A., Slemr, F., Brenninkmeijer, C. A. M., and Ziereis, H.: Pollution events observed during CARIBIC flights in the upper troposphere between South China and the Philippines, Atmos. Chem. Phys., 10, 1649–1660, doi:10.5194/acp-10-1649-2010, 2010.

Lämmerzahl, P., Röckmann, T., Brenninkmeijer, C. A. M., Krankowsky, D., and Mauersberger, K.: Oxygen isotope composition of stratospheric carbon dioxide, Geophys. Res. Lett., 29, 1582, doi:1510.1029/2001GL014343, 2002.

Levin, I., Allison, C., Brand, W., Conway, Delmotte, M., Facklam, C., Francey, R., Hammer, S., Huang, L., Jordan, A., Langenfelds, R., Machida, T., Meijer, H., Mukai, H., Neubert, R., Sabasch, M., Schmidt, M., Steele, P., Steinberg, B., Ramonet, M., Rothe, M., Vaughn, B., and Worthy, D.: Five Years of International Flask Intercomparison (Sausage Flask ICP) 2002–2007, 14th WMO/IAEA Meeting of Experts on Carbon Dioxide Concentration and Related Tracers Measurement Techniques, Helsinki, Finland, 10–13 September 2007, available online at: http://www.fmi.fi/research_climate/climate_7.html, (last access: September 2010), 2007.

Levin, I. and Karstens, U.: Inferring high-resolution fossil fuel CO_2 records at continental sites from combined $^{14}CO_2$ and CO observations, Tellus B, 59, 245–250, doi:10.1111/j.1600-0889.2006.00244.x, 2007.

Levin, I., Hammer, S., Kromer, B., and Meinhardt, F.: Radiocarbon observations in atmospheric CO_2: Determining fossil fuel CO_2 over Europe using Jungfraujoch observations as background, Sci. Total Environ., 391, 211–216, doi:10.1016/j.scitotenv.2007.10.019, 2008.

Lintner, B. R., Buermann, W., Koven, C. D., and Fung, I. Y.: Seasonal circulation and Mauna Loa CO_2 variability, J. Geophys. Res., 111, D13104, doi:10.1029/2005JD006535, 2006.

Masarie, K. A. and Tans, P. P.: Extension and integration of atmospheric carbon dioxide data into a globally consistent measurement record, J. Geophys. Res., 100, 11593–11610, 1995.

Masarie, K. A., Langenfelds, R. L., Allison, C. E., Conway, T. J., Dlugokencky, E. J., Francey, R. J., Novelli, P. C., Steele, L. P., Tans, P. P., Vaughn, B., and White, J. W. C.: NOAA/CSIRO flask air intercomparison experiment: A strategy for directly assessing consistency among atmospheric measurements made by independent laboratories, J. Geophys. Res., 106, 20445–20464, 2001.

Matsueda, H., Machida, T., Sawa, Y., Nakagawa, Y., Hirotani, K., Ikeda, H., Kondo, N., and Goto, K.: Evaluation of atmospheric CO_2 measurements from new flask air sampling of JAL airliner observations, Pap. Meteorol. Geophys., 59, 1-17, 2008.

Matsueda, H. H., Inoue, Y., and Ishii, M.: Aircraft observation of carbon dioxide at 8–13 km altitude over the western Pacific from 1993 to 1999, Tellus, 54B, 1–21, 2002.

Miller, J. B., Tans, P. P., White, J. W. C., Conway, T. J., and Vaughn, B. W.: The atmospheric signal of terrestrial carbon isotopic discrimination and its implication for partitioning carbon fluxes, Tellus B, 55B, 197-206, 2003.

Miyazaki, K., Patra, P. K., Takigawa, M., Iwasaki, T., and Nakazawa, T.: Global-scale transport of carbon dioxide in the troposphere, J. Geophys. Res., 113, D15301,

doi:10.1029/2007JD009557, 2008.

Miyazaki, K., Machida, T., Patra, P. K., Iwasaki, T., Sawa, Y., Matsueda, H., and Nakazawa, T.: Formation mechanisms of latitudinal CO_2 gradients in the upper troposphere over the subtropics and tropics, J. Geophys. Res., 114, 114, D03306, doi:10.1029/2008JD010545, 2009.

Nevison, C. D., Kinnison, D. E., and Weiss, R. F.: Stratospheric influences on the tropospheric seasonal cycles of nitrous oxide and chlorofluorocarbons, Geophys. Res. Lett., 31, L20103, doi:10.1029/2004GL020398, 2004.

Nevison, C. D., Mahowald, N. M., Weiss, R. F., and Prinn, R. G.: Interannual and seasonal variability in atmospheric N_2O, Global Biogeochem. Cy., 21, GB3017, doi:10.1029/2006GB002755, 2007.

Pan, L. L., Hintsa, E. J., Stone, E. M., Weinstock, E. M., and Randel, W. J.: The seasonal cycle of water vapor and saturation vapor mixing ratio in the extratropical lowermost stratosphere, J. Geophys. Res., 105, 26519–26530, 2000.

Pan, L. L., Randel, W. J., Gary, B. L., Mahoney, M. J., and Hintsa, E. J.: Definitions and sharpness of the extratropical tropopause: A trace gas perspective, J. Geophys. Res.-Atmos., 109, D23103, doi:10.1029/2004JD004982, 2004.

Pan, L. L., Bowman, K. P., Shapiro, M., Randel, W. J., Gao, R. S., Campos, T., Davis, C., Schauffler, S., Ridley, B. A., Wei, J. C., and Barnet, C.: Chemical behavior of the tropopause observed during the Stratosphere-Troposphere Analyses of Regional Transport experiment, J. Geophys. Res., 112, 112, D18110, doi:10.1029/2007JD008645, 2007.

Pan, L. L., Randel, W. J., Gille, J. C., Hall, W. D., Nardi, B., Massie, S., Yudin, V., Khosravi, R., Konopka, P., and Tarasick, D.: Tropospheric intrusions associated with the secondary tropopause, J. Geophys. Res., 114, D10302, doi:10.1029/2008JD011374, 2009.

Pataki, D. E., Ehleringer, J. R., Flanagan, L. B., Yakir, D., Bowling, D. R., Stil, C. J., Buchmann, N., Kaplan, J. O., and Berry, J. A.: The application and interpretation of Keeling plots in terrestrial carbon cycle research, Global Biogeochem. Cy., 17, 1022, doi:1010.1029/2001GB001850, 2003.

Patra, P. K. and Maksyutov, S.: Incremental approach to the optimal network design for CO_2 surface source inversion, Geophys. Res. Lett., 29(10), 1459, doi:10.1029/2001GL013943, 2002.

Patra, P. K., Maksyutov, S., Baker, D., Bousquet, P., Bruhwiler, L., Chen, Y.-H., Ciais, P., Scott Denning, A., Fan, S., Fung, I.Y., Gloor, M., Gurney, K., Heimann, M., Higuchi, K., John, J., Maki, T., Maksyutov, S., Peylin, P., Prather, M., Pak, B., Sarmiento, J., Taguchi, S., Takahashi, T., Yuen, C.-W.: Sensitivity of Optimal Extension of Observation Networks to the Model Transport, Tellus, 55B, 498–511, 2003.

Pupek M., Assonov, S. S., Mühle, J., Rhee, T. S., Oram, D., Koeppel, C., Slemr, F., and Brenninkmeijer, C. A. M.: Isotope analysis of hydrocarbons: trapping, recovering and archiving hydrocarbons and halocarbons separated from ambient air, Rapid Commun. Mass Sp., 19, 1–6, doi:10.1002/rcm.1812, 2005.

Quay, P., Sonnerup, R., Westby, T., Stutsman, J., and McNichol, A.: Changes in the $^{13}C/^{12}C$ of dissolved inorganic carbon in the ocean as a tracer of anthropogenic CO_2 uptake, Global Biogeochem. Cy., 17(1), 1004, doi:10.1029/2001GB001817, 2003.

Rayner, P. J., Law, R. M., Allison, C. E., Francey, R. J., Trudinger, C. M., and Pickett-Heaps, C.: Interannual variability of the global carbon cycle (1992–2005) inferred by inversion of at-

mospheric CO_2 and $^{13}CO_2$ measurements, Global Biogeochem. Cy., 22, GB3008, doi:10.1029/2007GB003068, 2008.

Rhee, T. S., Brenninkmeijer, C. A. M., Mühle, J., van Velthoven, P. F. J., Hermann, M., Zahn, A., Oram, D. E., Scharffe, D. H., Koeppel, C., Fischer, H., and Lelieveld, J.: A case study of rapid mixing across the extratropical tropopause based on Civil Aircraft for the Regular Investigation of the Atmosphere Based on an Instrumented Container (CARIBIC) observations, J. Geophys. Res.-Atmos., 110, D22301, doi:22310.21029/22005JD005890, 2005.

Schuck, T. J., Brenninkmeijer, C. A. M., Slemr, F., Xueref-Remy, I., and Zahn, A.: Greenhouse gas analysis of air samples collected onboard the CARIBIC passenger aircraft, Atmos. Meas. Tech., 2, 449–464, doi:10.5194/amt-2-449-2009, 2009.

Schuck, T. J., Brenninkmeijer, C. A. M., Baker, A. K., Slemr, F., von Velthoven, P. F. J., and Zahn, A.: Greenhouse gas relationships in the Indian summer monsoon plume measured by the CARIBIC passenger aircraft, Atmos. Chem. Phys., 10, 3965–3984, doi:10.5194/acp-10-3965-2010, 2010.

Shia, R.-L., Liang, M.-C., Miller, C. E., and Yung, Y. L.: CO_2 in the upper troposphere: Influence of stratosphere-troposphere exchange, Geophys. Res. Lett., 33, L14814, doi:10.1029/2006GL026141, 2006.

Still, C. J., Riley, W. J., Biraud, S. C., Noone, D. C., Buenning, N. H., Randerson, J. T., Torn, M. S., Welker, J., White, J. W. C., Vachon, R., Farquhar, G. D., and Berry, J. A.: Influence of clouds and diffuse radiation on ecosystem-atmosphere CO_2 and $CO^{18}O$ exchanges, J. Geophys. Res., 114, G01018, doi:10.1029/2007JG000675, 2009.

Stohl, A., Spichtinger-Rakowsky, N., Bonasoni, P., Feldmann, H., Memmesheimer, M., Scheel, H. E., Trickl, T., Hübener, S., Ringer, W., and Mandl, M.: The influence of stratospheric intrusions on alpine ozone concentrations, Atmos. Environ., 34, 1323–1354, 2000.

Stohl, A., Bonasoni, P., Cristofanelli, P., Collins, W., Feichter, J., Frank, A., Forster, C., Gerasopoulos, E., Gaggeler, H., James, P., Kentarchos, T., Kromp-Kolb, H., Kruger, B., Land, C., Meloen, J., Papayannis, A., Priller, A., Seibert, P., Sprenger, M., Roelofs, G. J., Scheel, H. E., Schnabel, C., Siegmund, P., Tobler, L., Trickl, T., Wernli, H., Wirth, V., Zanis, P., and Zerefos, C.: Stratosphere-troposphere exchange: A review, and what we have learned from STACCATO, J. Geophys. Res., 108(D12), 8516, doi:10.1029/2002JD002490, 2003.

Strahan, S. E., Douglass, A. R., Nielsen, J. E., and Boering, K. A.: The CO_2 seasonal cycle as a tracer of transport, J. Geophys. Res.-Atmos., 103, 13729–13741, 1998.

Turnbull, J. C., Miller, J. B., Lehman, S. J., Tans, P. P., Sparks, R. J., and Southon, J.: Comparison of $^{14}CO_2$, CO, and SF_6 as tracers for recently added fossil fuel CO_2 in the atmosphere and implications for biological CO_2 exchange, Geophys. Res. Lett., 33, L01817, doi:10.1029/2005GL024213, 2006.

Vaughn, B. H., Evans, C. U., White, J. W. C., Still C. J., Masarie, K. A, and Turnbull, J.: Global Network Measurements of Atmospheric Trace Gas Isotopes, in: Isoscapes: Understanding movement, pattern, and process on Earth through isotope mapping, edited by: West, J. B., Bowen, G. J., Dawson, T. E., and Tu, K. P., XXIV, 3–31, ISBN-978-90-481-3353-6, Springer Science + Business Media B. V., 3–31, 2010.

VIM 3: International vocabulary of metrology - Basic and general concepts and associated terms, VIM, 3rd edition, JCGM 200:2008, available at: http://www.bipm.org/en/publications/guides/vim.html, (last access: September 2010), 2008.

White, J. W. C. and Vaughn, B. W.: University of Colorado, Institute of Arctic and Alpine Research (INSTAAR), Stable Isotopic Composition of Atmospheric Carbon Dioxide (^{13}C and ^{18}O) from the NOAA ESRL Carbon Cycle Cooperative Global Air Sampling Network, 1990–2007, Version: 1 June 2009, Path: ftp://ftp.cmdl.noaa.gov/ccg/co2c13/flask/event/, 2009.

Zahn, A., Brenninkmeijer, C. A. M., Asman, W. A. H., Crutzen, P. J., Heinrich, G., Fischer, H., Cuijpers, J. W. M., and van Velthoven, P. F. J.: Budgets of O_3 and CO in the upper troposphere: CARIBIC passenger aircraft results 1997–2001, J. Geophys. Res.-Atmos., 107(D17), 4337, doi:10.1029/2001JD001529, 2002.

Zahn, A., Brenninkmeijer, C. A. M., and van Velthoven, P. F. J.: Passenger aircraft project CARIBIC 1997-2002 – Part II: the ventilation of the lowermost stratosphere, Atmos. Chem. Phys. Discuss., 4, 1119–1150, doi:10.5194/acpd-4-1119-2004, 2004a.

Zahn, A., Brenninkmeijer, C. A. M., and van Velthoven, P. F. J.: Passenger aircraft project CARIBIC 1997-2002 – Part I: the extratropical chemical tropopause, Atmos. Chem. Phys. Discuss., 4, 1091–1117, doi:10.5194/acpd-4-1091-2004, 2004b.